

Spring 2011

Identifying novel proteins in translation complex by using analytical ultracentrifugation with fluorescent detection system

Chongxu Zhang

University of New Hampshire, Durham

Follow this and additional works at: <https://scholars.unh.edu/dissertation>

Recommended Citation

Zhang, Chongxu, "Identifying novel proteins in translation complex by using analytical ultracentrifugation with fluorescent detection system" (2011). *Doctoral Dissertations*. 578.
<https://scholars.unh.edu/dissertation/578>

This Dissertation is brought to you for free and open access by the Student Scholarship at University of New Hampshire Scholars' Repository. It has been accepted for inclusion in Doctoral Dissertations by an authorized administrator of University of New Hampshire Scholars' Repository. For more information, please contact nicole.hentz@unh.edu.

**IDENTIFYING NOVEL PROTEINS IN TRANSLATION
COMPLEX BY USING ANALYTICAL
ULTRACENTRIFUGATION WITH FLUORESCENT
DETECTION SYSTEM**

BY

CHONGXU ZHANG

Master's Degree, Shaanxi Normal University, 2004

DISSERTATION

**Submitted to the University of New Hampshire
in Partial Fulfillment of
the Requirements for the Degree of**

Doctor of Philosophy

in

Biochemistry

May, 2011

UMI Number: 3467373

All rights reserved

INFORMATION TO ALL USERS

The quality of this reproduction is dependent upon the quality of the copy submitted.

In the unlikely event that the author did not send a complete manuscript and there are missing pages, these will be noted. Also, if material had to be removed, a note will indicate the deletion.



UMI 3467373

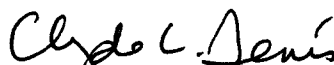
Copyright 2011 by ProQuest LLC.

All rights reserved. This edition of the work is protected against unauthorized copying under Title 17, United States Code.

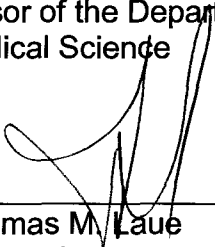


ProQuest LLC
789 East Eisenhower Parkway
P.O. Box 1346
Ann Arbor, MI 48106-1346

This thesis has been examined and approved.



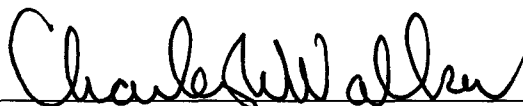
Dissertation Director, Dr. Clyde L. Denis
Professor of the Department of Molecular, Cellular and
Biomedical Science



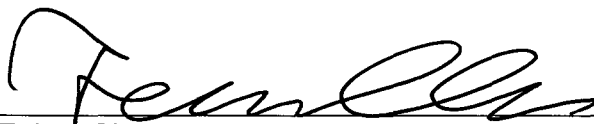
Dr. Thomas M. Laue
Professor of the Department of Molecular, Cellular and
Biomedical Science



Dr. W. Kelley Thomas
Hubbard Professor in Genomics and Director



Dr. Charles W. Walker
Professor of the Department of Molecular, Cellular and
Biomedical Science



Dr. Feixia Chu
Assistant Professor of the Department of Molecular,
Cellular and Biomedical Science

Date

ACKNOWLEDGEMENT

I am heartily thankful to my supervisor, Professor Clyde L. Denis, whose encouragement, guidance and support from the initial to the final level enabled me to develop an understanding of the subject. I would like to thank Professor Tomas Laue, Kelley Thomas, Charles Walker and Feixia Chu for their expert guidance and generous assistance, which helped me to make necessary improvements.

I am deeply indebted to the Dr. Yueh-Chin Chiang, Roy Richardson, and Xin Wang whose constant help and support allowed me to complete my project; I also need to thank Matthew Power, Shaun Toomey and other undergraduate students in our lab for their help and friendship. I offer my regards and blessings to all of the department and those who supported me in any respect during the completion of the project.

Last but not the least; I would like to thank my family. I cannot be what I am without my family who stand beside me in all my times.

TABLE OF CONTENTS

ACKNOWLEDGEMENT	III
LIST OF FIGURES	V
LIST OF TABLES	VII
ABSTRACT	VIII

CHAPTER	PAGE
1. GENERAL INTRODUCTION	1
2. MATERIALS AND METHODS	21
3. CHAPTER 3	26
4. CHAPTER 4	45
5. RESULTS DISCUSSION	91
6. SUMMARY	102
REFERENCES	105

LIST OF FIGURES

1. A typical structure of eukaryotic Messenger RNA	3
2. Deadenylation-dependent mRNA decay pathway	6
3. The current translation initiation model	8
4. A Sequence alignment of RRM1 domain	
B The mutations used for deadenylation assays	31
5. Sequence alignment of P domain	32
6. Diagram of GAL1 gene RNA	35
7. Northern analysis of GAL1 mRNA	35, 36
8. Structure of the Human PABP RRM1/2-RNA complex	39
9. Northern analysis of GAL1 mRNA.	40, 41
10. eIF4G and eIF4E were co-purified with Flag-PAB1	53
11. AUC analysis result of crude extracts	64
12. Sucrose gradient analysis of mRNP complexes	65
13. AUC analysis of the Flag-eluted material	66
14. AUC analysis of eIF4G1-GFP (A) and eIF4E-GFP (B) Flag pull down material	68
15. AUC analysis of PGK1 U1A-GFP (A) and RPS4B-GFP (B) Flag pull down material	71
16. Depletion of glucose reduce the signal RPS4B (A), eIF4E (B), eIF4G1 (C) at 78S complex	73, 74
17. AUC data analysis of 14 proteins (A-D) with formaldehyde treatment	77, 78
18. eIF4E level in each Flag pull down material	79
19. AUC data analysis of Flag pull down material with or without Flag (A-K)	82, 83
20. AUC data analysis of SUI2 and PRT1 without formaldehyde treatment	85
21. AU-FDS analysis for SBP1, SLF1, SUP35, SSD1, and PUB1 without formaldehyde treatment	87

LIST OF TABLES

1	Summary of eIF2 subunits	12
2	Summary of eIF3 subunits in <i>S. cerevisiae</i>	14
3	The summary of yeast eIF4 subunits	16
4	Strains and plasmids used in this study	24, 25
5	Proteins in the list were identified in 40% or less of the mass spectrometric experiments	58
6	List of 44 likely PAB1-associated proteins	59
7	List of proteins that were found to associate with PAB1 in relatively equivalent levels to that of eIF4G.	62
8	The 78S complex intensity reduction of glucose depletion compared to normal growth conditions for SBP1, SLF1, SUP35, SSD1, PUB1 in different experiments	88
9	S values for SBP1, SLF1, SSD1, PUB1, and SUP35 in 6 experiments	88

ABSTRACT

Identifying novel proteins in translation complexes by using analytical ultracentrifugation with fluorescent detection system.

by

CHONGXU ZHANG

University of New Hampshire, May, 2011

The primary components of the translation complex have been identified by a variety of techniques. However, it is likely that all components of the translation complex are still not fully discovered. Identifying new components should lead to a better understanding of the translation process and how it is regulated. Using mass spectrometric studies, we have identified 41 non-ribosomal proteins and non-translation initiation factors as possible components of the translation complex. To determine which of these proteins are in the translation complex, we applied analytical ultracentrifugation with fluorescent detection system (AU-FDS) to detect this complex. Following a one-step affinity purification with Flag-PAB1 using strains carrying translation factors and specific mRNA tagged with GFP, we identified the 78S translation complex that contains all of the major

components expected of the translation complex: mRNA, eIF4E, eIF4G1/eIF4G2, PAB1, 40S and 60S ribosomal components. Using GFP fused to about half of the 41 putative novel proteins of the components of the 78S translation complex, we were able to identify at five new proteins, SBP1, SLF1, PUB1, SUP35 and SSD1 as being part of this complex. SBP1 had previously been shown to be a component of stress granules formed following glucose depletion and SLF1 to be associated with translational process. PUB1 could bind to ARE and STE sequence. SUP35 was also reported in the 80S translation complex in 2008. SSD1 had a global effect on translation, and is found associate with the 5'-UTR of CLN2 mRNA. Components of the eIF3 and eIF2 α complex were also found to be part of the 78S complex, although formaldehyde cross-linking was required to stabilize their association with this complex. These results confirm the utility of AU-FDS for charactering the constitution of multi-subunit complexes and identified 5 new proteins in the 78S translation complex.

CHAPTER 1

GENERAL INTRODUCTION

Messenger RNA (mRNA) is transcribed from a DNA template and carries this information to the sites of protein synthesis, the ribosomes. Here, the nucleic acid polymer is translated into a polymer of amino acids: a protein. Proper and appropriate gene expression is essential to cellular processes ranging from following developmental cues to monitoring metabolic activity.

Since a translationally competent mRNA is absolutely required for the translation of protein, it is important to understand its structure and how mRNA is degraded. The structure of a mature eukaryotic mRNA includes the 5' cap, 5' untranslated regions (UTRs), start codon, coding sequence, stop codon, 3' untranslated regions, and poly(A) tail. A typical eukaryotic mRNA structure is shown in Figure 1.

The 5' cap is a 7-methylguanosine (m7G) residue attached backwards to the 5' end of the pre-mRNA using a 5'-5'-triphosphate linkage. This modification is critical for specifically binding of mRNA to the ribosome as well as protection from 5' exonucleases. Coding regions are composed of codons, which are decoded and translated to proteins by the ribosome. Coding regions begin with the start codon and end with a stop codon. Generally, the start codon is an AUG triplet and the stop codon is UAA, UAG, or UGA. The coding regions tend to be

stabilized by internal base pairs that impede degradation (Shabalina et al 2006, Katz et al 2003). In addition to being protein-coding, portions of coding regions may serve as regulatory sequences in the pre-mRNA as exonic splicing enhancers or exonic splicing silencers (Blencowe et al 2000). Several roles in gene expression have been attributed to the untranslated regions, including mRNA stability, mRNA localization, and translational efficiency. The ability of a UTR to perform these functions depends on the sequence of the UTR and can differ between mRNAs. Translational efficiency, sometimes including the complete inhibition of translation, can be controlled by UTRs. Proteins that bind to either the 3' or 5' UTR may affect translation by influencing the ribosome's ability to bind to the mRNA. MicroRNAs bound to the 3' UTR also may affect translational efficiency or mRNA stability. Some of the elements contained in untranslated regions form a characteristic secondary structure when transcribed into RNA. These structural mRNA elements are involved in regulating the mRNA. Some, such as the SECIS element (Mix et al 2006), are targets for specific proteins to bind. One class of mRNA element, the riboswitches (Wachter et al 2010), directly binds small molecules, changing their folding to modify levels of transcription or translation. In these cases, the mRNA regulates itself.

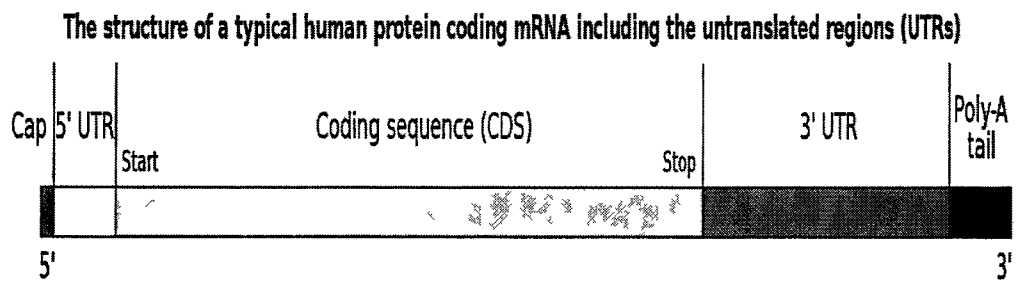


Figure 1, Legend: A typical structure of eukaryotic Messenger RNA

The 3' poly(A) tail is a long sequence of adenine nucleotides. The poly(A) promotes mRNA export from the nucleus and translation and protects the mRNA from degradation. In eukaryotes, mRNA molecules form circular structures due to an interaction between the cap binding complex and poly(A) -binding protein (Niehrs et al 1999). Poly(A) binding protein (PABP, also named PAB1 in yeast) was first isolated in 1973. *PAB1* is an essential gene but yeast strains carrying a *PAB1* deletion can be viable with certain translation defects, indicating that PAB1 plays critical functions in cell translation (Yao et al 2007). PAB1 consists of a highly conserved N terminus containing four tandem RNA recognition motifs (RRM1-4), an unstructured Proline and Methionine rich region (P), and a globular C-terminal region (C) (Sachs et al 1986). In addition, RRM2 binds eIF4G (Otero et al 1999). RRM4 is responsible for most of the nonspecific RNA binding of PAB1 (Kühn et al 1996). In yeast the first two of the RRMs are sufficient to confer viability to cells depleted of the normal *PAB1* gene. A single N-terminal domain is nearly identical to the entire protein in the number of high-affinity sites for poly(A) binding in vitro (one site with an association constant of approximately 2×10^7 M⁻¹) and in the size of the binding site (12 A residues), while wild-type yeast PAB1 protein approximately covers 25 A residues per molecule (Sachs et al 1987). The poly(A) binding protein (PAB1) interacts with eukaryotic initiation factor 4G (eIF4G), a component of the eIF4F complex, which binds to the 5' cap structure. The PAB1-eIF4G interaction brings about the circularization of the

mRNA by joining its 5' and 3' termini, thereby stimulating mRNA translation (Wells et al 1998).

Inside eukaryotic cells there is a balance between the processes of translation and mRNA decay. mRNA that are being actively translated are bound by ribosomes, the eukaryotic initiation factors eIF4E and eIF4G, and poly(A) - binding protein. eIF4E and eIF4G block the decapping enzyme (DCP2), and poly(A)-binding protein blocks the 3' degradation by deadenylase, such as CCR4-NOT complex (Chen et al 2001), thereby protecting the ends of the mRNA. Although most analyses of gene expression focus on transcriptional regulation, mRNA stability is an important factor in the control of gene expression, as mRNA degradation rates can vary over at least a 20 fold range (Decker et al 1993).

Degradation of the mRNA body occurs following deadenylation of the 3' end and decapping of the 5' 7-meG cap. Initial trimming of the poly(A) tail, down to 70-90 A's, in yeast is accomplished by the PAN2/PAN3 complex (Tucker M et al, 2002). The remaining A's are digested down to a size that PAB1 cannot bind, approximately 10 A's, by the catalytic component of the CCR4-NOT complex, CCR4 (Chen J et al, 2002). Disruption of the translation initiation complex, eIF4F, occurs when PAB1 disassociates from the poly(A) tail. Decapping requires DCP1 and DCP2, and additional proteins such as DHH1, EDC1, EDC2, LSM1-7, and PAT1 (Bouveret E, 2000; Bonnerot C, 2000; Dunckley T, 2001; Schwartz D, 2003). Following poly(A) tail removal and decapping, XRN1 then degrades the

mRNA in the 5' to 3' direction (Muhlrad D et al, 1994). Also, a multi-component complex, called the exosome, can digest the mRNA in the 3' to 5' direction after deadenylation (Mitchell P et al, 1997; Anderson JS et al, 1998). The two general pathways of mRNA decay and the proteins that act in them are shown in Figure 2.

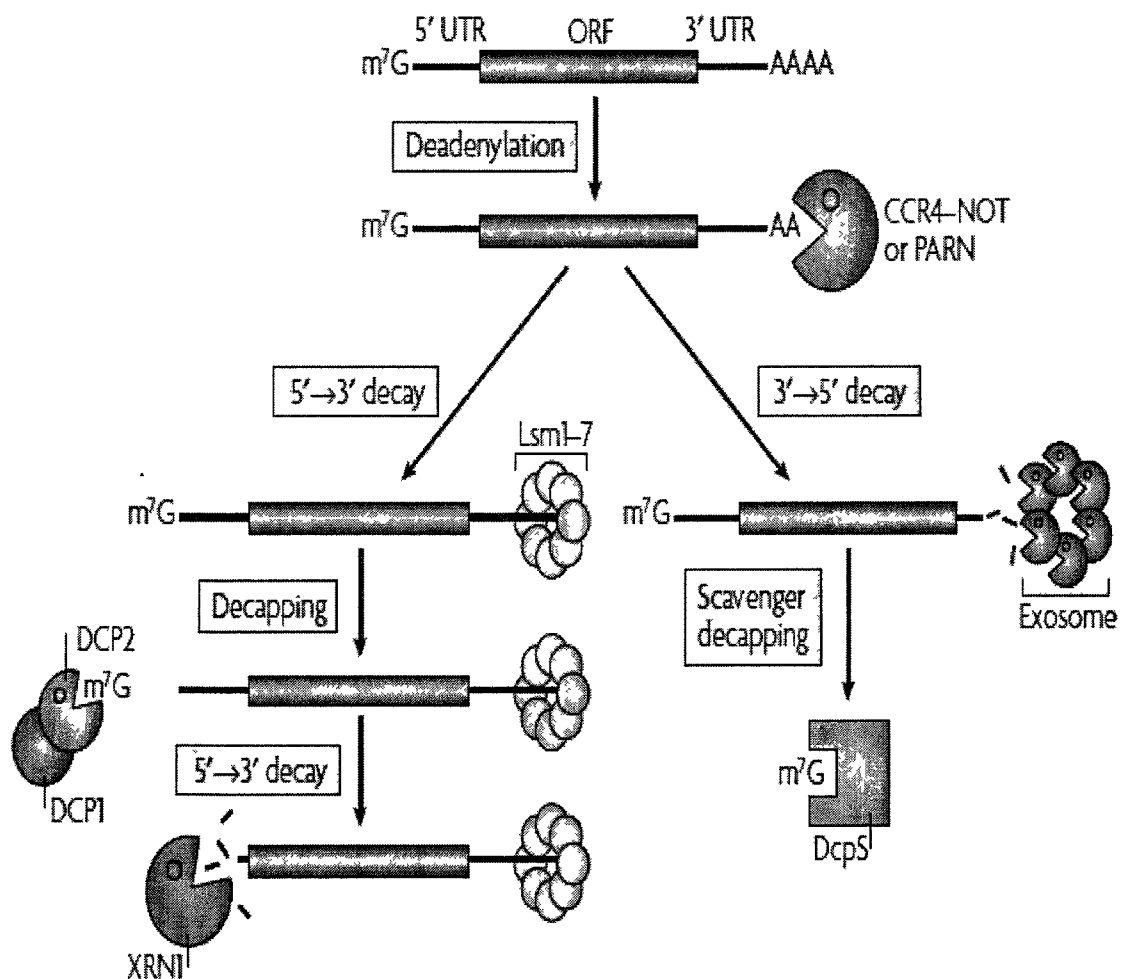


Figure 2, Legend: Deadenylation-dependent mRNA decay pathway.

Current translation initiation model

Of all the steps in mRNA translation, initiation is the one that differs most radically between prokaryotes and eukaryotes. In 1976, Pelham, et al developed the nuclease-treated rabbit reticulocyte lysate system for assaying translation of exogenous mRNAs. This system was able to translate all eukaryotic mRNAs accurately and efficiently, whether from yeast, insect, plant or mammalian cells, implying that all eukaryotes shared a common initiation mechanism (Pelham et al 1976). The initiation phase of protein synthesis does more than assemble the components that will polymerize. Selection of the start codon sets the reading frame that is maintained normally throughout all steps in the translation process. Protein synthesis is often regulated at the level of initiation, which adds to the importance of that step. The current translation initiation model is shown as Figure 3.

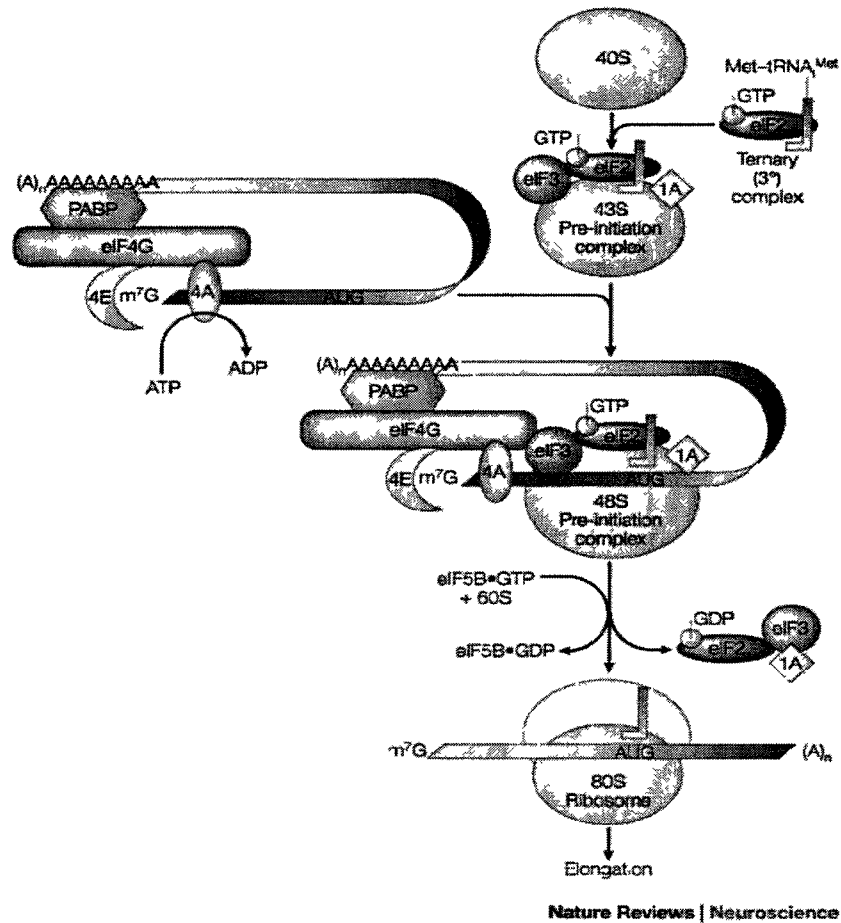


Figure 3, Legend: A binary complex of eukaryotic translation initiation factor 2 (eIF2) and GTP binds to methionyl-transfer RNA (Met-tRNA^{Met}), and the ternary complex associates with the 40S ribosomal subunit. The association of additional factors, such as eIF3 and eIF1A (1A), with the 40S subunit promotes ternary complex binding and generates a 43S pre-initiation complex. The cap-binding complex, which consists of eIF4E (4E), eIF4G and eIF4A (4A), binds to the 7-methyl-GTP (m⁷GTP) cap structure at the 5' end of a messenger RNA (mRNA). eIF4G also binds to the poly(A)-binding protein (PABP), thereby bridging the 5' and 3' ends of the mRNA. This mRNA circularization and the ATP-dependent helicase activity of eIF4A are thought to promote the binding of the 43S pre-initiation complex to the mRNA, which produces a 48S pre-initiation complex. Following scanning of the ribosome to the AUG start codon, GTP is hydrolysed

by eIF2, which triggers the dissociation of factors from the 48S complex and allows the eIF5B- and GTP-dependent binding of the large, 60S ribosomal subunit.

Proteins are assembled from amino acids using information encoded in genes.

Translation initiation begins with the binding of Met-tRNA_i^{Met} to the 40S ribosomal subunit in a ternary complex (TC) with eukaryotic initiation factor 2 (eIF2) and GTP. First, Met-tRNA_i^{Met} in a complex with eukaryotic initiation factor 2 (eIF2) and GTP, the ternary complex (TC), bind to the 40S ribosome, creating the 43S preinitiation complex (PIC) in a reaction stimulated by eIF1, eIF1A, eIF3, and eIF5 (Algire et al 2002). The mRNA, prebound to the cap-binding complex eIF4E, eIF4G and the poly(A) binding protein, then binds to the 43S PIC to form the 48S PIC. The 48S PIC scans the mRNA for AUG start codon; the GTP in the TC is hydrolyzed at this time in a reaction stimulated by eIF5. The eIF2-GDP is released from the 40S ribosome, leaving Met-tRNA_i^{Met} in the P site (Hershey et al 2000). Finally, joining of the 60S ribosomal subunit occurs in a reaction stimulated by eIF5B (Pestova et al 2000), and the remaining initiation factors dissociate from the resulting 78S initiation complex (Unbehaun et al 2004).

Translation initiation factors (IFs)

There are many non-ribosomal proteins called initiation factors (IFs, or for eukaryotes, eIFs) that promote and regulate the formation of the translation initiation complex. At least 28 different polypeptides (aggregate >1600 kDa) are involved in translation initiation in mammalian cells, which is actually larger than

the size of the 40S ribosomal subunit (Richard 2005). The known factors include eIF1 through 6.

eIF1 has two subunits, eIF1 and eIF1A. One of the first functions attributed to eIF1 and eIF1A was facilitating TC binding to the 40S ribosome. In addition, eIF1 and eIF1A facilitate recruitment of one another by binding cooperatively to the 40S subunit (Maag et al 2003). Genetic studies have identified Sui- mutants of eIF1A, as well as mutants that read through a start codon, a phenotype called leaky scanning (Fekete et al 2005). The leaky scanning phenotype of the eIF1A mutants and the ability of eIF1 to suppress initiation at non-AUG codons suggested that eIF1 and eIF1A might act in antagonistic ways, with eIF1 being responsible for preventing premature engagement with putative start codons and eIF1A facilitating pausing at the correct start codon long enough to proceed with downstream initiation events (Sarah F et al 2008).

eIF2 has three subunits, eIF2- α , β , and γ . The primary role of eIF2 in translation initiation is to transfer Met-tRNA_i^{Met} to the 40S ribosomal subunit. (Pain VM et al 1996) Following the association of mRNA with the 40S subunit and location of the subunit at the AUG start codon, eIF5 binds to eIF2 and stimulates the hydrolysis of eIF2-bound GTP. The α -subunit contains a serine at position 51, which is a phosphate acceptor for three protein kinases: heme-regulated inhibitor (HRI), double-stranded RNA-activated protein kinase (PKR), and the nutrient-

regulated protein kinase (GCN2). Yeast eIF2 α additionally contains three casein kinase II (CK-II) sites in the C-terminal region which are not conserved in the mammalian protein (J. van den et al 1995). The β -subunit contains three lysine clusters in the N-terminal domain (NTD) which are important for the interaction with eIF2B. The γ -subunit comprises three guanine nucleotide binding sites and is known to be the main docking site for GTP/GDP (Roll-Mecak et al 2004).

Subunit	Alpha	Beta	Gamma
Molecular Weight / kDa	36	38	52
Similarity	eIF2-alpha family	GTP-binding elongation factor family	eIF2-beta / eIF5 family
Interactions		Binding of eIF5, eIF2B and RNA	Binding of GTP and RNA

Table 1, Legend: Summary of eIF2 subunits.

eIF3 is the largest scaffolding initiation factor. There are 13 nonidentical subunits in the mammalian cell, designated eIF3a to eIF3m. In contrast, yeast contains only five orthologs of mammalian eIF3 subunits, eIF3a, eIF3b, eIF3c, eIF3g and eIF3i (Phan L et al 1998), all of which are essential for translation in vivo (Asano et al 1998). Most of the reactions in the initiation pathway are stimulated by eIF3, including assembly of the eIF2–GTP–Met-tRNA_i^{Met} ternary complex (TC), binding of TC and other components of the 43S PIC to the 40S subunit, mRNA recruitment to the 43S PIC complex, and scanning the mRNA for AUG recognition (Hinnebusch 2006). eIF3 can bind to 40S ribosomes in the absence of other eIFs and can prevent the association of the 60S subunit with the 40S subunit. This function of eIF3 is dependent on other factors including the TC (Kolupaeva et al 2005).

eIF3 can stimulate 43S PIC assembly. Yeast eIF3, eIF1, eIF5 and TC can be isolated in a multifactor complex (MFC) free of 40S subunits (Asano K et al 2000). Yeast strain expressing unstable forms of eIF2b, eIF3a plus eIF3b, and eIF5 have shown that completely depleting each factor reduces 40S binding by all other MFC constituents (Jivotovskaya AV et al 2006).

Name	Standard Name	Molecular Weight (Da)	Isoelectric Point (pI)	function
eIF3a	Rpg1p	110,343	6.24	subunit of the core complex of translation initiation factor 3 (eIF3), essential for translation; part of a subcomplex (Prt1p-Rpg1p-Nip1p) that stimulates binding of mRNA and tRNA(i)Met to ribosomes
eIF3b	Prt1p	88,129	5.88	subunit of the core complex of translation initiation factor 3 (eIF3), essential for translation; part of a subcomplex (Prt1p-Rpg1p-Nip1p) that stimulates binding of mRNA and tRNA(i)Met to ribosomes
eIF3c	Nip1p	93,203	4.69	subunit of the eukaryotic translation initiation factor 3 (eIF3), involved in the assembly of the preinitiation complex and start codon selection
eIF3g	Tif35p	30,501	6.78	subunit of the core complex of translation initiation factor 3 (eIF3), which is essential for translation
eIF3i	Tif34p	38,755	5.48	subunit of the core complex of

				translation initiation factor 3 (eIF3), which is essential for translation
--	--	--	--	---

Table 2, Legend: Summary of eIF3 subunits in *S. cerevisiae*.

eIF4 initiation factors include eIF4A, eIF4B, eIF4E, and eIF4G. eIF4F is often used to refer to the complex of eIF4A, eIF4E, and eIF4G. Yeast does not have clear orthologs of mammalian eIF4B subunits. The summary of yeast eIF4 subunits are shown in Table 3. eIF4E, the mRNA 5' cap binding protein, and eIF4A, an ATP-dependent RNA helicase, bind the large scaffolding protein, eIF4G, which contains binding domains for mRNA, PABP and eIF3. The closed-loop model proposes that eIF4G's ability to tether the 5' mRNA cap (via eIF4E) to the poly(A) tail (via PABP) greatly increases translation efficiency (Derry et al 2006). It is also proposed that the closed-loop structure may facilitate ribosome recycling during termination stage of translation of the mRNA (Von der Haar et al 2004).

Name	Gene Name	Molecular Weight (Da)	Isoelectric Point (pI)	function
eIF4A	TIF1, TIF2	44,697	4.85	Translation initiation factor eIF4A, identical to Tif1p; DEA(D/H)-box RNA helicase that couples ATPase activity to RNA binding and unwinding; forms a dumbbell structure of two compact domains connected by a linker; interacts with eIF4G
eIF4E	CDC33	24,254	5.25	Cytoplasmic mRNA cap binding protein and translation initiation factor eIF4E; the eIF4E-cap complex is responsible for mediating cap-dependent mRNA translation via interactions with translation initiation factor eIF4G (Tif4631p or Tif4632p)
eIF4G1	TIF4631	107,101	5.91	Translation initiation factor eIF4G, subunit of the mRNA cap-binding protein complex (eIF4F) that also contains eIF4E (Cdc33p); interacts with PAB1 and with eIF4A (Tif1p); also has a role in biogenesis of the large ribosomal subunit
eIF4G2	TIF4632	103,898	7.69	Translation initiation factor eIF4G, subunit of the mRNA cap-binding protein complex (eIF4F) that also contains eIF4E (Cdc33p); associates with the poly(A)-binding protein PAB1, also interacts with eIF4A (Tif1p); homologous to Tif4631p

Table 3, Legend: The summary of yeast eIF4 subunits

eIF5 includes eIF5A and eIF5B. eIF5A is a GTPase-activating protein, which helps the large ribosomal subunit associate with the small subunit. It is required for GTP-hydrolysis by eIF2 and contains the unusual amino acid hypusine (Park MH 2006). eIF5B is a GTPase, and is required for general translation initiation by promoting Met-tRNA_i^{Met} binding to ribosomes and ribosomal subunit joining; It is a homolog of bacterial IF2.

eIF6 is one constituent of 66S pre-ribosomal particles, and has similarity to human translation initiation factor 6 (eIF6). It appears to be involved in the biogenesis and/or stability of 60S ribosomal subunits. eIF6 is necessary for both ribosome biogenesis and translation, indicating it could mediate a continuum between the maturation of the large 60S subunit in the nucleus and translation in the cytoplasm (Miluzio A et al 2006). The initiation factor eIF6 is also involved in tumorigenesis, although its involvement is insufficiently characterized. For example, eIF6 is abundant in colon cancers (Sanvito et al 2000) and aggressive leukemia (Harris et al 2004).

Translational regulation

Translation initiation regulation is the key step in the control of protein synthesis, as control of translation initiation allows a rapid and dynamic cellular response to environment change. Two established regulatory mechanisms target distinct steps in translation initiation. First, the formation of the closed loop mRNP complex can be inhibited either by eIF4E-binding proteins (4E-BPs) or by eIF4E homologous proteins (4EHPs). 4E-BPs competitively inhibits the eIF4G–eIF4E interaction thereby preventing translation initiation either in a global or mRNA-specific manner. *Saccharomyces cerevisiae* has two 4E-BPs, Caf20p and Eap1p, which transnationally regulate some mRNAs, yet are unlikely to act as global translational regulators (Ibrahimo et al 2006). A second regulated step in the translation initiation pathway involves activation of the stress-responsive eIF2 α kinases. The initiator methionyl tRNA (Met-tRNA_i^{Met}) forms a ternary complex (TC) with eIF2-GTP and is recruited to the 40S ribosome. GTP hydrolysis generates eIF2-GDP as a byproduct of translation initiation, and this is recycled to eIF2-GTP by a guanine nucleotide exchange factor, eIF2B. Phosphorylation of eIF2 by the eIF2 α kinases inhibits this recycling to reduce the level of TC, which ultimately limits translation initiation (Kapp et al 2004). The yeast eIF2 α kinase Gcn2p responds in this manner to stresses such as amino acid starvation (Hinnebusch, 2005). In addition, other means of effecting the translation initiation can be imagined including controlling 43S binding to the closed loop structure.

Appropriate regulation of mRNA translation is essential for growth and survival; and translation is controlled by a complex set of mechanisms acting at multiple levels, ranging from global protein synthesis to individual mRNAs (Mehta et al 2010). The components of translation initiation complex are still not fully discovered. For example, almost all aspects of the mechanism of ribosomal scanning remain uncharacterized (Pestova et al 1999). It is possible that ribosomal scanning on longer or more highly structured 5' - nontranslated region may require additional as-yet-unidentified factors, for example to enhance processivity or to promote unwinding of stable secondary structures (Tatyana et al 2001). The subject of my thesis is to identify new components in the translation initiation complex. The previous research in our lab indicated that we could specifically co-immunoprecipitate the closed-loop structure in yeast by using a PAB1 tagged at its N-terminus with the Flag peptide. Both eIF4G and eIF4E were found to co-elute with PAB1 (shown in Figure 4). This fundamental result makes it possible to identify new components in the purified material by mass spectrometric analysis. However, determining the size of the protein complex identified by mass spectrometric analysis requires additional methods. Analytical ultracentrifugation (AUC) has proven to be a primary method for determining molecular weight and molecular size of proteins for several decades (MacGregor et al 2004). Xin Wang (Ph. D student in our laboratory) showed that AUC analysis of crude extracts subjected to a one step affinity purification could identify yeast translation complexes by using Flag-PAB1. Furthermore, she

identified 78S complex that decreased about 7 fold in abundance following glucose depletion, a condition that causes rapid translational stoppage (Ashe et al, 2000). This co-relationship indicated we could identify new components in the 78S translational complex by using AUC analysis.

To identify new components in the translation complex, we first purified the PAB1 associated complex by using Flag-PAB1 immunoprecipitation, and subjected purified material to mass spectrometric analysis. From this analysis we identified 41 non-ribosomal proteins and non-translation initiation factors as possible components of the poly(A) binding protein (PAB1) mRNP structure and of translation initiation complex. Based on their stoichiometry association with PAB1, 25 of these proteins were likely to be present in translation complexes. To determine which of these proteins were in the translation complex, we applied analytical ultracentrifugation with fluorescent detection system (AU-FDS) to detect this complex. Using GFP fused to 25 of these putative novel proteins of the components of the 78S translation complex, we were able to identify five new proteins, SBP1, SLF1, PUB1, SUP35 and SSD1, as being part of this complex.

CHAPTER 2

MATERIALS AND METHODS

Yeast strains and growth conditions

Saccharomyces cerevisiae strain AS319 (*MAT α ade2 ura3 leu2 trp1 his3 pab1::HIS3 pAS77 [PAB1-CEN-URA3]*) was used for transforming PAB1 variants expressed under their own promoter on plasmid YC504 (*pRS314:PAB1-CEN-TRP1*) as indicated in (Yao et al 2007). Plasmid AS77 was subsequently lost from each strain following selection on plates containing 5-fluoroorotic acid.

For the AUC analysis, strains expressed C-terminally tagged GFP- fusion proteins (Table 4) in conjunction with a Flag peptide tagged at the N-terminus/C-terminus of PAB1 or a Flag peptide tagged at the C-terminus of RPL25A (RPL25A-Flag).

Cell lysis and Flag purification

FLAG peptide (N-DYKDDDDK-C): 25 mg / ml stock in lysis buffer. Cells were grown in appropriate liquid media to mid-log phase (OD_{600} 1.0~1.2) and harvested at 7000 rpm for 6 minutes. Two volumes of ice-cold lysis buffer (1X Lysis buffer: 50mM Tris, 150mM KCl, 2mM Mg^{2+} , 10% glycerol, pH 7.5), with yeast protease inhibitor cocktail with a protease inhibitor cocktail (Sigma) and two volume of glass beads. The cells were lysed by multiple vortexing (9 times) at highest speed for 1 minute, followed by resting on ice 1 minute. The lysed cells

were centrifuged for 10 minutes at 14000 rpm to pellet the cellular debris. The supernatant was transferred to a new tube and a 250 ul of Flag beads was added and vortexed for 4 hours at 4°C. After washing the packed gel with lysis buffer, most of the wash buffer was removed without discarding the resin and spun at 3000 rpm for 5 minutes. The supernatant was decanted and discarded. This procedure was repeated four times. 250 ul of lysis buffer was added to Flag beads with 200 ug/ml of Flag peptide and the samples were incubated with gentle shaking for 30 minutes at 4°C. The resin was centrifuged for 5 minutes at 4000 rpm. The supernatants were transferred to fresh test tubes without disturbing the resin. Elution was repeated one more time and the combined collected sample was then used for further analysis.

In vivo formaldehyde (HCHO) cross-linking

Cells was grown to OD 600 1.0~1.2 in appropriate medium and transferred to precooled centrifuge bottles that contain 25% of the total culture volume of crushed ice (50 g ice per 200 ml of culture) to quickly cool the cells by inverting the centrifuge bottle five times. HCHO from a 37% stock solution was added to a final concentration of 1% relative to the original volume of the culture (5.4 ml 37% HCHO per 200 ml culture) to the cooled cells by inverting the centrifuge bottle 10 times and leaving the bottle on wet ice for 1 hour. HCHO cross-linking was stopped by the adding of glycine to a final concentration of 0.1 M, from a 2.5 M stock solution. After cross-linking with HCHO and addition of glycine, the cells

were collected by centrifugation (6 minutes at 7000 rpm). The cells were washed by resuspending the cell in 20 ml of ice cold lysis buffer.

Analytical Ultracentrifugation and Western-blot

The Flag purified sample was loaded into a centrifuge cell, allow to equilibrium at 20°C for about one hour and then run in the centrifuge at 15000 rpm. After 200 scans, the data was collected and analyzed by using sedenfit software (version: v12p1).

Western-blot

Western blots were conducted for each Flag pull-down preparation to establish that equivalent levels of material were subjected to AU-FDS analysis (eIF4E and PAB1 levels were assessed). A 6 X sodium dodecyl sulfate (SDS) polyacrylamide gel electrophoresis loading buffer [375mM Tris, pH 6.8, 12% SDS, 30% sucrose, 0.06% bromophenol blue, and 1.47% 2-mercaptoetethanol] was added to samples to a final dilution of 1:6 and the samples were boiled for 10 minutes, prior to SDS-polyacrylamide gel electrophoresis and Western blot analysis (Jivotovskaya et al 2006).

Strain	Genotype	Origin
CBC1-GFP	<i>MAT a leu2 ura3 his3 met15 CBC1-GFP (HIS)</i>	Huh et al 2003
elF4E-GFP	<i>MAT a leu2 ura3 his3 met15 EIF4E-GFP (HIS)</i>	Brengues et al 2003
elF4G1-GFP	<i>MAT a leu2 ura3 his3 met15 EIF4G1-GFP (HIS)</i>	Brengues et al 2003
GBP2-GFP	<i>MAT a leu2 ura3 his3 met15 GBP2-GFP (HIS)</i>	Huh et al 2003
GCD11-GFP	<i>MAT a, ADE2, his3-11, 15, leu2-3, 112, trp1-1, ura3-1, can1-100, GCD1-P180, GCD11-GFP::G418</i>	Susan et al 2005
GCD6-GFP	<i>MAT a, ADE2, his3-11, 15, leu2-3, 112, trp1-1, ura3-1, can1-100, GCD1-P180 GCD6-GFP::G418</i>	Susan et al 2005
HRP1-GFP	<i>MAT a leu2 ura3 his3 met15 HRP1-GFP (HIS)</i>	Huh et al 2003
LHP1-GFP	<i>MAT a leu2 ura3 his3 met15 LHP1-GFP (HIS)</i>	Huh et al 2003
MFA2 U1A-GFP	<i>MAT a leu2-3, 112 trp1 ura3-52 prt1-63 cup1::LEU2/PGK1pG/MFA2pG U1A-GFP (NEO)</i>	Huh et al 2003
NAB3-GFP	<i>MAT a leu2 ura3 his3 met15 NAB3-GFP (HIS)</i>	Huh et al 2003
NAB6-GFP	<i>MAT a leu2 ura3 his3 met15 NAB6-GFP (HIS)</i>	Huh et al 2003
PBP1-GFP	<i>MAT a leu2-3, 112 trp1 ura3-52 his4-539 cup1::LEU2/PGK1pG/MFA2pG PBP1-GFP (NEO)</i>	Buchan et al 2008
PBP2-GFP	<i>MAT a leu2 ura3 his3 met15 PBP2-GFP (HIS)</i>	Huh et al 2003
PRT1-GFP	<i>MAT a, ADE2, his3-11, 15, leu2-3, 112, trp1-1, ura3-1, can1-100, GCD1-P180, PRT1-GFP::G418</i>	Susan et al 2005
PUB1-GFP	<i>MAT a leu2 ura3 his3 met15 PUB1-GFP (HIS)</i>	Huh et al 2003
RPS4B-GFP	<i>MAT a leu2 ura3 his3 met15 RPS4B-GFP (HIS)</i>	Huh et al 2003
RRP12-GFP	<i>MAT a leu2 ura3 his3 met15 RRP12-GFP (HIS)</i>	Huh et al 2003
RRP5-GFP	<i>MAT a leu2 ura3 his3 met15 RRP5-GFP (HIS)</i>	Huh et al 2003
SBP1-GFP	<i>MAT a his3Δ1 leu2Δ0 met15Δ0 ura3Δ0 SBP1-GFP (NEO)</i>	Scott et al 2006
SGN1-GFP	<i>MAT a leu2 ura3 his3 met15 SGN1-GFP (HIS)</i>	Huh et al 2003
SLF1-GFP	<i>MAT a leu2 ura3 his3 met15 SLF1-GFP (HIS)</i>	Huh et al 2003
SMB1-GFP	<i>MAT a leu2 ura3 his3 met15 SMB1-GFP (HIS)</i>	Huh et al 2003

SSD1-GFP	<i>MAT a leu2 ura3 his3 met15 SSD1-GFP (HIS)</i>	Huh et al 2003
SUI2-GFP	<i>MAT a, ADE2, his3-11, 15, leu2-3, 112, trp1-1, ura3-1, can1-100, GCD1-P180 SUI2-GFP::G418</i>	Susan et al 2005
SUP35-GFP	<i>MAT a leu2 ura3 his3 met15 SUP35-GFP (HIS)</i>	Huh et al 2003
UPF1-GFP	<i>MAT a leu2 ura3 his3 met15 UPF1-GFP (HIS)</i>	Huh et al 2003
XRN1-GFP	<i>MAT a leu2-3,112 ura3-52, trp1Δ63 XRN1-GFP (Neo)</i>	Teixeira et al 2005
YGR250c-GFP	<i>MAT a leu2 ura3 his3 met15 YGR250C-GFP (HIS)</i>	Huh et al 2003
Plasmids		
pRP1 659	<i>Pab1-GFP, Edc3-mCh; Cen; TRP1 marker</i>	Buchan et al 2008
pRP1 657	<i>Pab1-GFP, Edc3-mCh; Cen; URA3 marker</i>	Buchan et al 2008

Table 4, legend: Strains and plasmids used in this study.

CHAPTER 3

Introduction

Degradation of the mRNA body occurs following deadenylation of the 3' end and decapping of the 5' 7-meG cap. Initial trimming of the poly(A) tail, down to 70-90 A's, in yeast is accomplished by the PAN2/PAN3 complex (Tucker et al 2002). The remaining A's are digested down to a size that PAB1 cannot bind, approximately 10 A's, by the catalytic component of the CCR4-NOT complex, CCR4 (Chen et al 2002).

CCR4-NOT complex and PAB1 regulates the deadenylation

The *CCR4* gene was initially identified by Clyde L. Denis in 1984 in which mutations in *CCR4* blocked depression of the *ADH2* gene (Denis CL 1984). In 2001 *CCR4* was discovered to be responsible for the majority of mRNA deadenylation in the cell. Additional components of the CCR4-NOT complex are CAF1, NOT1-5, CAF40, CAF130, and BTT1 (Chen J et al 2002, Cui et al 2008). Genetic evidence also suggests a CCR4-NOT complex involvement in transcriptional elongation (Denis et al 2001). *CCR4* has a typical leucine rich repeat between 365–433 that is necessary for its association with CAF1 and the other components of the CCR4-NOT complex. The C-terminal domain of *CCR4* is important for *CCR4* activities that are both RNA and single stranded DNA 30 – 50 exonuclease activities, with a preference for 30 poly(A) substrates (Chen et al 2002, Viswanathan et al 2004). Interestingly, this domain when overexpressed

as a fusion to LexA can partially complement the non-fermentative growth defect of a cell lacking CCR4 suggesting it might be an independent domain of the protein (Chen et al 2002).

Disruption of the translation initiation complex occurs when PAB1 dissociates from the poly(A) tail. Decapping ensues at this time and requires DCP1 and DCP2, and additional proteins such as DHH1, EDC1, EDC2, LSM1-7, and PAT1 (Schwartz et al 2003). Following poly(A) tail removal and decapping, XRN1 then degrades the mRNA in the 5' to 3' direction (Muhlrad et al 1994). Also, a multi-component complex, called the exosome, can digest the mRNA in the 3' to 5' direction after deadenylation (Mitchell et al 1997; Anderson et al 1998).

Several observations suggest that deadenylation is the rate limiting step of mRNA degradation. First, sequences promoting rapid degradation also promote increased deadenylation (Decker and Parker, 1993; LaGrandeur and Parker, 1999). Second, stable transcripts have a much slower deadenylation rate compared to transcripts that degrade rapidly (Decker and Parker, 1993; LaGrandeur and Parker, 1999). Lastly, decapping does not occur until the poly(A) tail is approximately 8-12 A's, which is the minimal length of poly(A) that PAB1 can bind (Decker and Parker, 1993; Sachs et al., 1987).

The PAB1 protein and its specific domains seem to have discrete functions in translation and deadenylation, as suggested by three observations. First, Sachs and colleagues have shown that RRM2 is involved in contacting eIF4G (Otero et

al 1999), which is also a core component of the mRNP complex (Wells et al 1998). The fact that the PAB1 RRM2 domain contacts eIF4G and that PAB1 RRM1 may not be directly involved in eIF4G contact while still having a role in translation suggests PAB1 RRM1 and PAB1 RRM2 each have different roles in translation. Second, each of the PAB1 RRMs have varying mRNA binding specificities and translational involvement (Burd et al 1991), also indicating a modular nature to the PAB1 protein. RRM1 and RRM2 bind most strongly to poly(A). Third, deletion of the RRM1 domain had a greatest effect on translation in vivo than did deletion of any of the other PAB1 domains (Yao et al 2007).

Since deletion of PAB1 is lethal and the various domains seem to serve different functions from one another, analysis of the PAB1 protein containing a deletion of each domain has been one way to better understand the function of the individual PAB1 domains and hence how the PAB1 protein functions. PAB1 domain deletions have been constructed and analyzed for various effects (Otero et al 1999; Yao et al 2007). PAB1 variants with RRM1 or P domain deletion were defective in deadenylation of several different mRNA indicating that the RRM1 and P domains of PAB1 might affect deadenylation in vivo (Yao et al 2007, Lee et al 2010). Our homology analysis for PAB1 (Darren Lee, previous Ph.D student in our lab) showed a number of conserved amino acid residues in RRM1 domain indicating that these residues might play important roles in the deadenylation process (Figure 4). To test which of these amino acid residues affect deadenylation we created PAB1 mutations for each of these amino acid

residues. Pulse-chase analysis was therefore conducted to determine the rates of mRNA deadenylation using each of these RRM1 variants.

On contrast, the construction of mutation across the P domain did not seem to be a feasible approach to analyzing its function because of the highly variable nature of the P domain across species. For example, ePAB (for embryonic poly(A) -binding protein), from the frog (*Xenopus*), is primarily expressed in embryonic cells. The N-terminal region that includes RRM1~4, are 82% identical to PAB1, while the C-terminal region of ePAB is significantly more divergent, with only 56% identity to PABP1 (Gia et al 2001). The mRNA expressed in these cells will not be degraded when ePAB is present. Similarly, in human T cells, iPABP (PABPC4 or iPABP) shows 79% sequence identity to PABP at the amino acid level. The RNA binding domains of iPABP and PABP are nearly identical, while their C termini are much more divergent (Yang et al 1995). iPABP is localized primarily to the cytoplasm. It is suggested that PABPC4 might be necessary for regulation of stability of labile mRNA species in activated T cells. iPABP may also be involved in the regulation of protein translation in platelets and megakaryocytes or may participate in the binding or stabilization of polyadenylates in platelet dense granules (database: Entrez Gene). Homology analysis for P domain of PAB1 is shown in Figure 5.

On this section, we hypothesized that ePABP and iPABP, with their aberrant P domains, contribute to stabilizing the mRNA to which they are bound. To test our hypothesis, we created three yeast PAB1 variants with P domain substitutions, i.e., PAB1-eP which the P domain from ePABP was substituted for that of PAB1, PAB1-iP replaced the P domain of wild type PAB1 with that of iPABP, and the PAB1-hP in which the P domain of human PABPC1 replaced the that of PAB1. Pulse-chase analysis was used for determination of the rates of mRNA deadenylation with each of these constructions.

A

Human-PABPC1	ASLYVGDLEPSVSEAHLYDI FSPIGSVSSIRVCRDAITKSLGYAYVNFNDHEAGRAIEQLNYTPIKGRICRIMWSQR
Xenopus-PABPC1	ASLYVGDLEPSVSEAHLYDI FSPIGSVSSIRVCRDAITKSLGYAYVNFNDHEAGRAIEQLNYTPIKGRICRIMWSQR
Human-PABPC4	ASLYVGDLEPSVSEAHLYDI FSPIGSVSSIRVCRDAITKSLGYAYVNFNDHEAGRAIEQLNYTPIKGRICRIMWSQR
Yeast-PAB1	ASLYVGDLEPSVSEAHLYDI FSPIGSVSSIRVCRDAITKSLGYAYVNFNDHEAGRAIEQLNYTPIKGRICRIMWSQR
Clustal Consens	*****

B

	β1										β2										β3										β4																																																																															
	40 50 60 70 80 90 100 110																																																																																																													
Human-PABPC1	ASLYVGDLEHPDVTEAMLYEKEFSPAGFILSIRICRELITSGSSNYAYVNFQHTKDAEHALDTMNFEDVIKGPVRIMWSQR																																																																																																													
Yeast-PAB1	ASLYVGDLEPSVSEAHLYDIFSPIGSVSSIRVCRDAITKTSLGAYVNFNDHEAGRKAIEQLNYTPIKGRICRIMWSQR																																																																																																													
	A A H D K A L A A N R K A A D E T D V A A A																																																																																																													

Figure 4, Legend: **A**, RRM1 sequence alignment of PABPC1 protein (16358990, Homo sapiens), Pabpc1 protein (30353795, Xenopus laevis), PABPC4 protein (66267552, Homo sapiens), and Pab1p protein (603406, Saccharomyces cerevisiae). The RRM1 domains are gray color residues between the black color residues as shown. The RRM1 domains of first three proteins are from 12 to 86. RRM1 within Pab1p protein is from 40 to 113. The consensus symbol "*" means that the residues are identical in all sequences in the alignment, ":" means that conserved substitutions have been observed and "." means that semi-conserved substitutions are observed. **B**, RRM1 sequence alignment of PABPC1 protein with PAB1 protein. RRM1 contains four β -sheets, showing as β 1- β 4 (Deo et al 1999). The amino acid residues numbers of PAB1 are showed above the sequences. The mutations used for deadenylation assays are pointed out by vertical lines and the group mutations exist in same strains is linked together as shown.

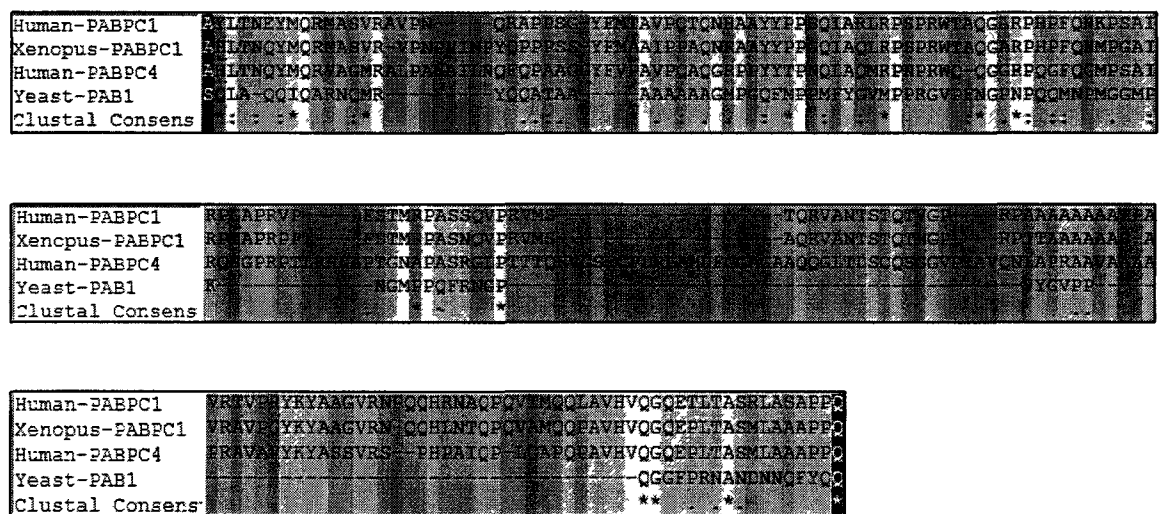


Figure 5, Legend: Sequence alignment of PABPC1 protein (16358990, Homo sapiens), Pabpc1 protein (30353795, Xenopus laevis), PABPC4 protein (66267552, Homo sapiens), and Pab1p protein (603406, Saccharomyces cerevisiae). The P domain within PAB1 protein is from 406 to 502, showing as gray residues between black residues. "-" represents gap position in the alignment. The consensus symbol "*" means that the residues are identical in all sequences in the alignment, ":" means that conserved substitutions have been observed and "." means that semi-conserved substitutions are observed.

Results

P domain substitutions do not affect the deadenylation rate in vivo. We examined directly the effect of PAB1 variants with P domain substitution on *GAL1* mRNA deadenylation rates by using pulse-chase experiments (Tucker et al 2001; Viswanathan et al 2004). Two *GAL1* mRNA species are produced in vivo that result from differential poly(A) site usage and differ by 110 nt in their 3' UTR (Miyajima et al 1984; Cui and Denis 2003). Following a brief induction of *GAL1* mRNA synthesis with addition of galactose to the medium, mRNA synthesis was shut off with glucose. The 3' ends of *GAL1* mRNA were detected by using an RNase H assay and a DNA probe that

was complementary to sequences present in both species. Two polyadenylated species migrating at about 380 and 275 nucleotides (nt) that corresponded to poly(A) sites at about 160 bp and 50 bp, respectively, downstream of the *GAL1* stop codon were identified (Figure 6). Each mRNA species contained about 80 nt of poly(A), as determined by a deadenylation assay (Tucker et al 2001). As shown in Figure 7, for wild type yeast PAB1, the oligo (A) species for *GAL1*-L began to occur around 6 min and is very much present by 10 min in agreement with our previous results (Yao et al 2007). For PAB1-hP, some oligo (A) species for *GAL1*-L was visible at 6 min and was definitely present at 10 min.

Densitometric analysis of these distribution is shown in Figure 6. On regards to *GAL1*-S, PAB1-hP appears to be slightly slowing its deadenylation rate. In the PAB1 background *GAL1*-S display significant oligo (A) species by 20 min but in

the PAB1-hP background this species began to be showed at 20 min and is greater abundance at 30 min. (Figure 5, top right panel). PAB1-eP showed very similarly to PAB1-hP in its effect on *GAL1-L* and *GAL1-S*. For *GAL1-S*, longer exposure (not shown) indicated that the oligo (A) form began to appear at 20 min and was very abundant at 30 min. On the contrast, to the above results, PAB1-iP displayed delayed deadenylation of *GAL1-L*, as the oligo (A) form did not appear until 15 min. However, a similar decrease in deadenylation rate was not observed on *GAL1-S*. Overall, these results suggest that at least P domains play similar roles in mRNA deadenylation in yeast.

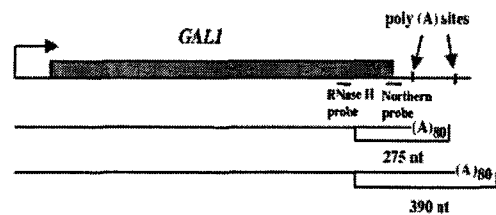
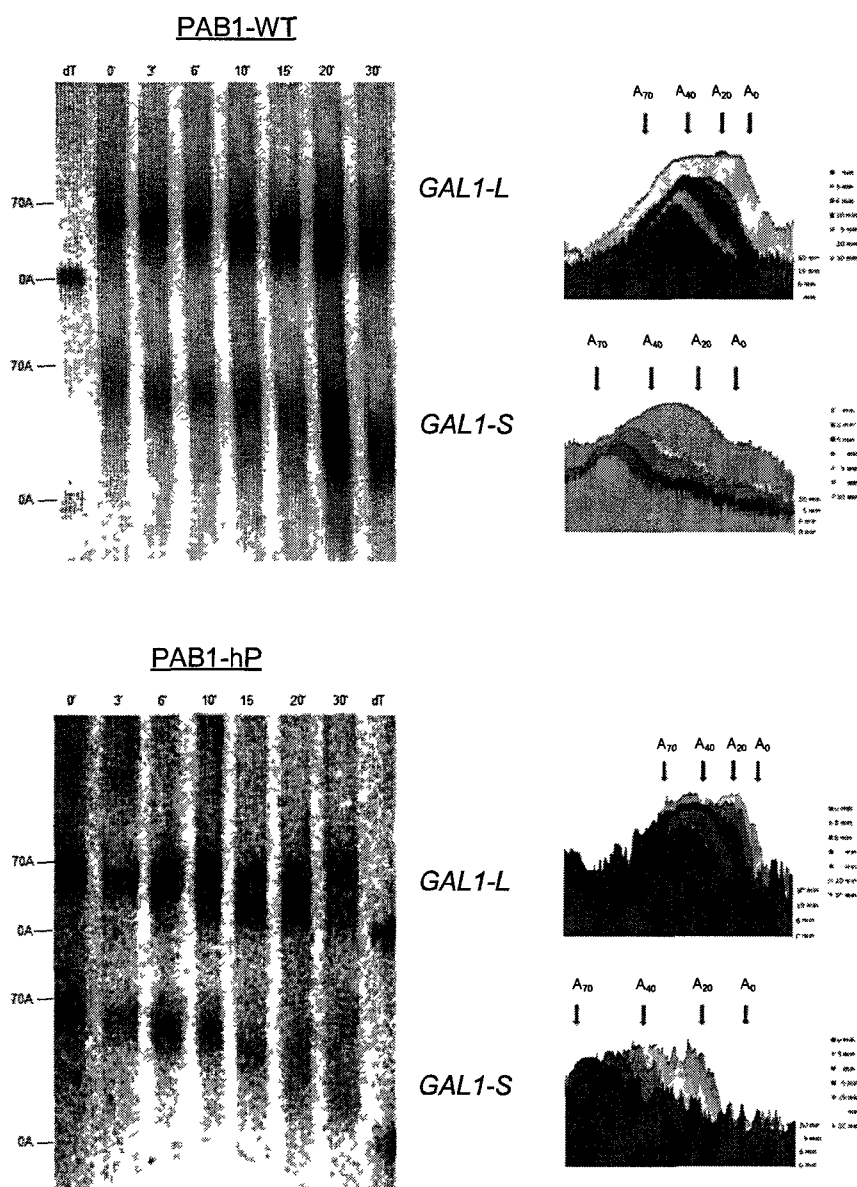


Figure 6, Legend: Diagram of GAL1 gene RNA. The two poly(A) sites located 50 and 160 bp downstream of the stop codon are indicated, as are the RNase H probe and the Northern probe.



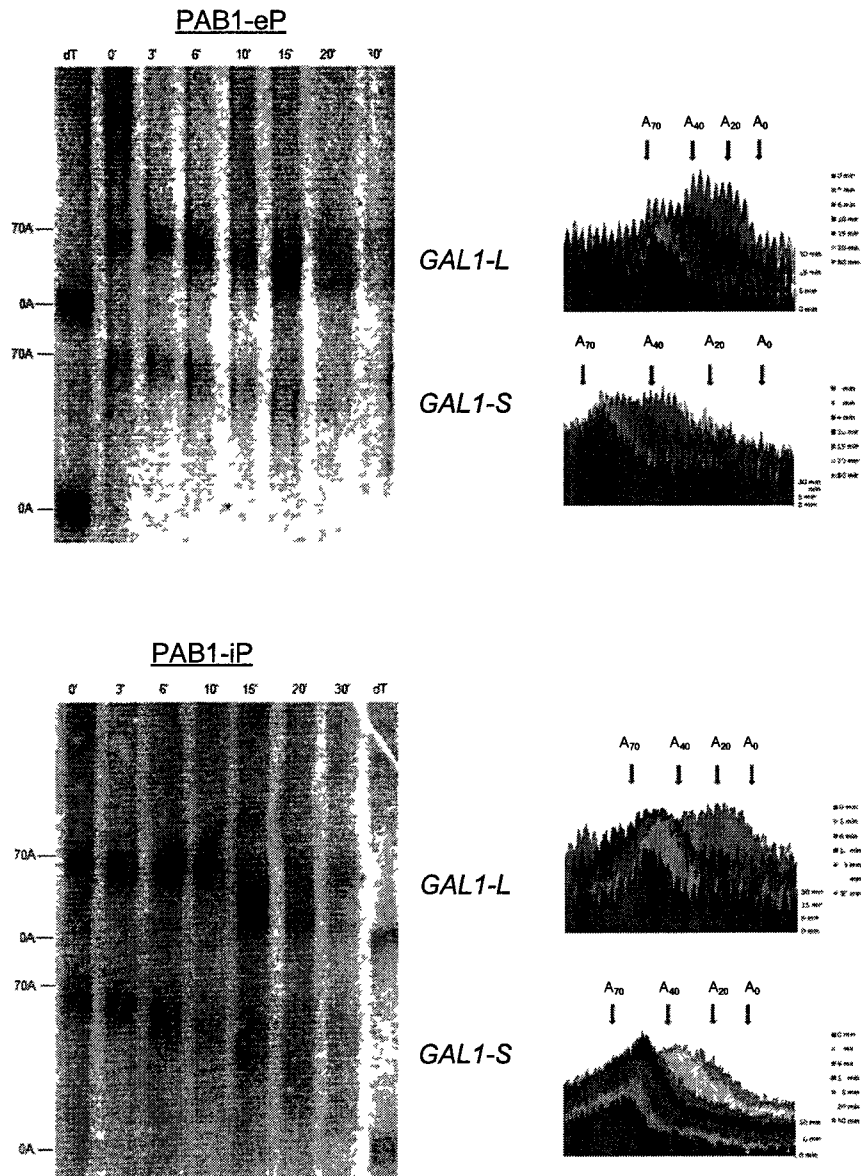


Figure 7, Legend: Northern analysis of GAL1 mRNA. Yeast was induced by galactose-containing medium for 8 min, followed by glucose addition, samples were collected at different time points (times are in minute), upon which total RNA was extracted. The poly(A) tail lengths are indicated. dT-RNA sample, which had been pretreated with oligo d(T) and RNase to remove the poly(A) tail prior to Northern analysis. Densitometric scans of each Northern blot are present in the right panels.

RRM1 point mutations affect the deadenylation rate in vivo

RRM1 and RRM2 share similar structures, these two RRM domains form a continuous RNA-binding trough, lined by an antiparallel β sheet backed by four α helices (shown in Figure 8). Because deletion of the RRM1 domain slowed deadenylation in vivo, we were interested in identifying particular residues important to this protein. Previously, we had mutated Y83V of RRM1 and shown that deadenylation was slowed (Yao et al 2007). To further identify residues we scanned the RRM1 domain for regional homology (Figure 7). PAB1 homology analysis (done by Darren Lee) showed many conserved amino acid residues in the RRM1 domain (Figure 4). These conserved residues are probably important for the function of PAB1 in mRNA turn over and other process. However, we did not wish to mutate only highly conserved residues, as many of these might be structural in nature. Mutation of them might disrupt the total function of the RRM1 domain. Therefore, we constructed two type of mutation. The first group were highly conserved residues in the β sheet RNA binding surface of RRM1. Since we have previously shown that mutation one such residue, Y83V, blocks deadenylation, we wished to target other such residues to verify if other mutations in the poly(A) binding surface of RRM1 slowed deadenylation. The second group of mutation involved those on the external surface of RRM1 not involved in RNA binding. Our reasoning in this case that residues on the surface of RRM2 have been shown to be important to its function (Otero et al 1999). These residues were identified by displaying compare lack of conservation

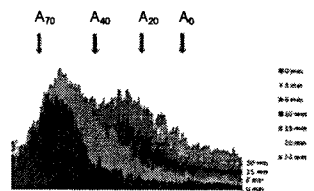
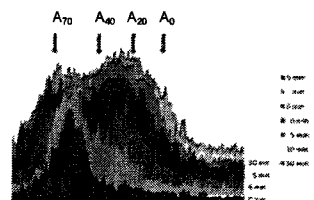
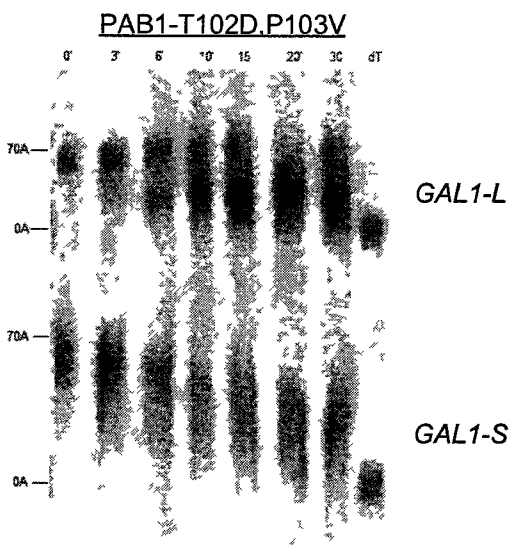
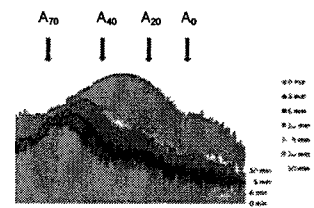
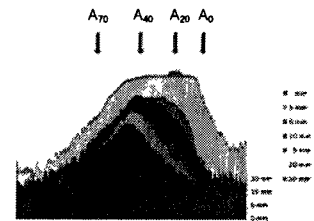
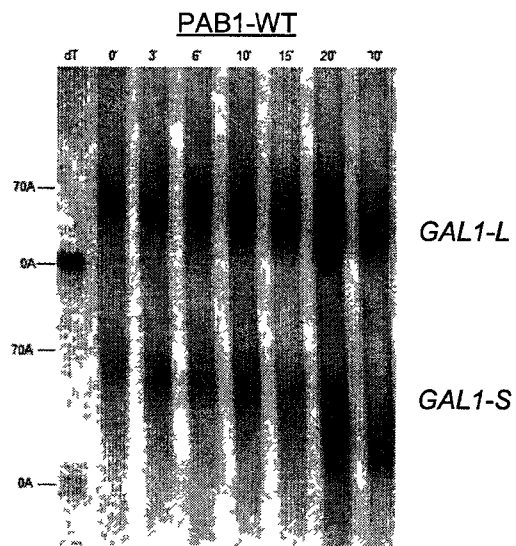
between human and yeast RRM1 sequence. As shown in Figure 8A, we showed nine individual or clusters of mutation that displayed difference between human and yeast sequence. We presumed that such difference might mediate residues whose protein binding consistent had changed between yeast and human. If this were the case, based on Otero et al 1999, we would be identifying regions on the RRM1 extenal non-RNA binding surface. That was making contact to other proteins, possibly those involved in mRNA deadenylation. The location of these mutations across the RRM1 domain are shown in Figure 8A. I analyzed three of these, {A91D, R93E}, {T102D, P103V}, and {R110A}. The other were analyzed by Darren Lee and Roy Richardson. Among this other group only Y41A had a dramatic decrease on deadenylation (not shown).

Following a brief induction of *GAL1* mRNA synthesis with addition of galactose to the medium, mRNA synthesis was shut off with glucose, and the length of *GAL1* mRNA poly(A) tail was followed as a function of time by Northern analysis. As shown in Figure 9, PAB1-A91D, R93E and PAB1-R110A showed no apparent differences in deadenylation from that of wild type PAB1, the oligo A species appear at 10 min for *GAL1*-L the same as wild type PAB1. PAB1-T102D, P103V showed faster deadenylation. Oligo A species appeared at 6 min for *GAL1*-L. Longer adenylated species also existed at this time and later times indicated a processive deadenylation of CCR4. *GAL1*-S deadenylation was also noticeably faster with PAB1-T102D, P103V in which oligo (A) species were found apparent

at 6 min. Again, long and short poly(A) species were showed for *GAL1-S*, indication of a processive deadenylation process. See Figure 9.



Figure 8, Legend: Structure of the Human PABP RRM1/2–RNA Complex (Deo et al 1999)
stereo drawing showing the extended RNA-binding surface created by approximation of RRM1
(red) and RRM2 (blue).



Discussion

The PAB1 protein binds the poly(A) tail of mRNA and plays roles in controlling mRNA production, export from the nucleus, translation into proteins, deadenylation, and decapping. A considerable amount of research has been conducted to identify the functional domains of PAB1. While the function and structure of the RNA binding regions of PAB1 have been somewhat characterized, one particular region of PAB1 remains obscure: the P domain. ePAB is expressed under conditions when the normal PABPC is not expressed and embryonic cells are defective in mRNA deadenylation (Voeltz et al 2001). Similarly, iPAB is highly expressed in T cells under conditions when lymphokine mRNAs are synthesized and particularly stabilized (Lindstein et al 1989). Here we tested if P domain affect the deadenylation rate in yeast and our results showed that it does not affect the GAL-1 deadenylation in vivo. The possible model is that ePAB and iPAB1 could interact with special proteins or other factors and by this way to stabilize the mRNA which they binding to. In yeast, absence of these kinds of factors may cause these P domain variants function no difference compare to wild type PAB1. Kim (Kim et al 2007) showed that ePAB transiently associates with the polyadenylation complex, it initially interacts with CPEB (cytoplasmic polyadenylation element binding protein), but after polyadenylation, it binds the poly(A) tail and stabilize the mRNA. The other possibility is that P domain plays no obvious role in deadenylation.

The RRM domains of PAB1 consist of four β -strands that form the RNA binding surface backed by two α -helices (Deo et al 1999). While RRM1 and RRM2 of PAB1 appear to bind most strongly to poly(A), RRM3 and RRM4 can also make critical contacts and may bind U-rich regions located adjacent to the poly(A) tail (Mullin et al 2004). The mRNA deadenylation process, catalyzed by the CCR4 deadenylase, is known to be the major factor controlling mRNA decay rates in *Saccharomyces cerevisiae*. Interestingly, the mutation (T102D, P103V) promotes the GAL1 deadenylation in a processive model.

The mechanism could be T102D, P103V mutation decrease the PAB1 binding ability to poly(A) tail and CCR4-Not complex is easier to access the poly(A) tail. This model can be tested by affinity assay.

Summary

The PAB1 domains seem to have discrete functions in translation. A considerable amount of research has been conducted to identify the functional domains of PAB1. The P domain is a proline-rich region that does not form any particular known structure. To further characterize the function of the P domain, I tested hybrid yeast PAB1 proteins that contain P domains from ePAB, iPAB and human PABP. Although ePAB and iPAB were reported that they can stabilize the mRNA which they bond to, the P domain variants function almost same as wild type PAB1 from our northern-blot assay. It is possible that certain factors can interact with ePAB and iPAB through P domain in their original cell but the factors do not exist in yeast. Another possibility is that P domain itself plays no important role in deadenylation process.

The RRM1 and RRM2 show almost same affinity compare to full length PAB1. Our previous data reveal conserved amino acid residues in these domains. These residues may be critical for PAB1's function. Our lab made a serial of mutation related to these residues and I analyzed three of them. The northern blot results showed that the mutations (R110A) and (A91D, R93E) do not affect deadenylation rate of GAL1 mRNA in vivo. The mutation (T102D, P103V) promotes deadenylation rate in a processive manner. These data indicate that T102 and P103 are important for PAB1 function and the mutation may reduce the affinity of PAB1 therefore promote mRNA turn over.

CHAPTER 4

Identifying novel proteins in translation initiation complexes by using analytical ultracentrifugation with fluorescent detection system.

Introduction

Defining protein complexes is critical to virtually all aspects of cell biology. Among different possible approaches to studying proteins, mass spectrometry (MS)-based proteomics is increasingly used to acquire the data important for understanding these processes. This technology is rapidly advancing and in modern proteomics it has essentially completely replaced previous tools such as two-dimensional gel electrophoresis (Walther et al 2010). MS is a way to accurately measure the weight of a molecule or more accurately its mass-to-charge ratio (m/z). Because mass analysis uses electromagnetic fields in a vacuum, molecules must first be electrically charged and transferred into the gas phase. Once in the gas phase, the m/z ratio of molecules is determined by their trajectories in a static or dynamic electric field. The mass differences between different proteins with similar composition is small and entire proteins are anyway difficult to measure (McLafferty et al 2007). Therefore, peptides derived from them by enzymatic cleavage are measured. The advantages of MS-based proteomics are that it focuses on proteins, their localization, modifications, and

interactions. It is also now becoming available to a larger community. One limitation is that interaction data from immunoprecipitation experiments reflect a population of protein complexes with unknown topologies. Information concerning pairwise protein interactions cannot be reliably obtained from these MS analyses.

Analytical ultracentrifugation (AUC) has proven to be a powerful method for characterizing solutions of macromolecules and an indispensable tool for the quantitative analysis of macromolecular interactions for over 75 years (Howlett et al 2006; Scott et al 2005).

Two complementary views of solution behavior are available from AUC. Sedimentation velocity (SV) provides first-principle, hydrodynamic information about the size and shape of molecules (Laue et al 1999). Sedimentation equilibrium (SE) provides first principle, thermodynamic information about the solution molar masses, stoichiometries, association constants, and solution nonideality (Howlett et al 2006; Laue 1995). The range of molecular weights suitable for AUC exceeds that of any other solution technique from a few hundred Daltons (e.g., peptides, dyes, oligosaccharides) to several hundred-million Daltons (e.g., viruses, organelles).

Absorbance is the most frequently used detector for the analytical ultracentrifuge (Laue 1996). The fluorescence optical system is the most recent addition to The Beckman Coulter XLI analytical ultracentrifuge (MacGregor et al 2004). Due to the extraordinary sensitivity and selectivity of fluorescence detection, it is possible to characterize the sedimentation behavior of GFP-labeled proteins in cell lysates without further purification (Kroe 2005). Fluorescence detectors make AUC applicable to a wide variety of questions in cell biology. In particular, the fluorescence system provides a new way to extend the scope of AUC to probe the behavior of biological molecules under physiological conditions.

The advantages of AUC analysis are several. First, in contrast to many commonly used methods, during AUC, samples are characterized in their native state under biologically relevant solution conditions. AUC provides useful information on the size and shape of macromolecules in solution with very few restrictions on the sample or the nature of the solvent. Second, analytical ultracentrifugation is a primary technique that is nondestructive, rapid, and simple. It can analyze up to 14 samples at one time and finish scans in a few hours (about 3~6 hours). Commonly-used methods to detect the size of protein complexes, such as chromatography or sucrose gradient analysis, require time-intensive western blot analysis to ensure what the peak is and what components are in the peak. In addition, AUC is at least an order of magnitude better at

resolving complexes than sucrose gradient analysis. AUC analysis takes several hundred analyses across a centrifuge run; sucrose gradient analysis is limited to take one 'scan' of the resultant centrifugation process.

The green fluorescent protein (GFP) was discovered in the course of bioluminescence studies of the hydrozoan jellyfish *A. victoria* (Shimomura et al 1962). The protein is composed of 238 amino acid residues (26.9kDa), which exhibits bright green fluorescence when exposed to blue light (Tsien 1998). GFP has a typical beta barrel structure, consisting of one β -sheet with alpha helix(s) containing the chromophore running through the center (Yang et al 1996). Inward facing sidechains of the barrel induce specific cyclization reactions in the tripeptide Ser65–Tyr66–Gly67 that lead to chromophore formation. The tightly packed nature of the barrel excludes solvent molecules, protecting the chromophore fluorescence from quenching by water (Ormö et al 1996). The GFP gene has been introduced and expressed in many bacteria, yeast and other fungi, fish (such as zebrafish), plant, fly, and mammalian cells, including human. Martin Chalfie, Osamu Shimomura, and Roger Y. Tsien were awarded the 2008 Nobel Prize in chemistry on 10 October 2008 for their discovery and development of the green fluorescent protein.

The proper control of translation, mRNA degradation, and the subcellular localization of mRNAs is a key aspect of gene expression regulation in eukaryotic cells. Over the past few years, it has emerged that cytosolic mRNAs are in a dynamic equilibrium between different functional and subcellular locations. Translating mRNAs can be found in polysomes, whereas nontranslating mRNAs often accumulate in either stress granules or P bodies (Parker and Sheth 2007). P-bodies are distinct foci within the cytoplasm of the eukaryotic cell consisting of many enzymes involved in mRNA turnover. P-bodies have been demonstrated to play fundamental roles in general mRNA decay, nonsense-mediated mRNA decay, AU-rich element mediated mRNA decay, and microRNA induced mRNA silencing. Stress granules have been primarily studied in mammalian cells and are dynamic aggregates of untranslating mRNAs in conjunction with a subset of translation initiation factors (eIF4E, eIF4G, eIF4A, eIF3, and eIF2), the 40S ribosomal subunit, and the poly(A) binding protein (Anderson and Kedersha 2006). Buchan and Parker (2008) showed P bodies promote stress granule assembly in *Saccharomyces cerevisiae*. In their model, mRNAs exiting translation may first enter P bodies, and undergo a similar sorting process resulting in either mRNA decay, storage in a translationally silenced state, or a return to translation via a stress granule mRNP state. The stress of glucose deprivation leads to a rapid loss of polysomes (Brenques et al 2005). This results in a rapid inhibition of protein synthesis and can be readily reversed upon readdition of glucose (McMahon et al 1995, Ashe et al 2000). Neither the

inhibition nor the reactivation of translation requires new transcription. This inhibition also does not require activation of the amino acid starvation pathway or inactivation of the TOR kinase pathway (Ashe et al 2000).

We successfully purified one or more mRNP complexes by co-immunoprecipitation with Flag-PAB1. Mass spectrometric analyses were conducted to identify the protein components in this Flag pull down material. Importantly, we conducted two sets of control experiments to eliminate contaminating proteins and identify proteins within the mRNP complex. By this way, we identified 44 proteins in our purified mRNP complex. After stoichiometric determination of the relative abundance of these 44 proteins, we identified 25 putative proteins which were likely present in mRNP complexes.

Xin Wang's AUC analysis of the Flag pull down material identified a 78S complex containing the 80S ribosome and translation initiation factors eIF4E and eIF4G associated with mRNA. She also showed that the abundance of 78S complex decreased under different stress conditions, suggesting the 78S complex is translation complex (The average sedimentation coefficient of 12 experiments of eIF4E-GFP, and eIF4G1-GFP was 77.7, we name the complex the 78S complex.). Her results suggested that novel proteins identified by mass spectrometric analysis could be filtered for their presence in this 78S complex.

We used our 25 putative proteins each labeled with GFP to conduct AU-FDS analysis for each protein. This was done to identify if the proteins migrated around at 78S. If the protein migrated at 78S, then glucose depletion treatment was performed to determine if the complex disappeared with this stress as does the 78S complex. Using this methodology, we identified five new proteins in the 78S translation complex.

Results

Purification of the closed-loop structure using Flag-PAB1

It is well known that eIF4E, eIF4G and PAB1 interaction supports the notion of a closed loop mRNP (Wells et al 1998). Efficient translation initiation and optimal stability of most eukaryotic mRNAs depends on the formation of a closed loop structure and the resulting synergistic interplay between the 5' m7G cap and the 3' poly(A) tail (Amrani et al 2008). Previous studies in our lab showed proteins known to be associated with PAB1 could be co-purified using a PAB1 tagged at its N-terminus with the Flag peptide (Yao et al 2007). A typical example of this is displayed in Figure 10. This Western blot result showed eIF4G and eIF4E were co-purified with Flag-PAB1 (lane 2). The result indicated that by targeting Flag tagged PAB1 with an antibody we could successfully pull out the complex out of crude extracts and thereby could potentially identify unknown members of the complex through mass spectrometric analysis.



Figure 10, Legend: Cell extracts from strain carrying the Flag-PAB1 were bound to Flag beads, eluted with Flag peptide, and Western analysis was used to detect the proteins indicated in the Figure. Lane 1 represents cell extracts from strain carrying wild type PAB1 without Flag tag.

Mass spectrometric analysis to identify PAB1-mRNP protein

While a number of proteins are known to associate with PAB1 through previous mass spectroscopic experiments (Gavin et al 2002; Ho et al 2002), there were major limitations of these studies in regards to a protein like PAB1. Because of the nature of the proteome-wide approaches that were previously taken in these studies, adequate experimental controls were not able to be conducted for each individual mass spectrometric analysis and therefore it was difficult to determine which interaction were non-specific.

Two types of control experiments (done at least in duplicate) were conducted to eliminate contaminating proteins from the list of proteins interacting with PAB1. The first was to conduct mass spectrometric analysis on Flag bead purified material from a strain with PAB1 without the Flag tag. The second was to conduct mass spectrometric analysis on Flag bead purified material extracted from strains carrying the Flag-PAB1 following an extensive RNase A treatment. RNase A treatment eliminates PAB1 binding to the poly(A) tail, allowing us to identify only those proteins that associated with PAB1 within the context of the PAB1-mRNP structure.

Each control experiment was conducted with strains carrying either wild-type PAB1 (without the Flag tag) or with Flag-PAB1 (RNase A treatment) and compared with Flag-PAB1 (no RNase A treatment). The number of unique peptides detected for each protein present following the Flag pulls down experiment rather than the number of total peptides detected was compared between these samples. Significant bias can be introduced with the counting of the total peptides due to the fact that certain peptides are more readily detected by mass spectrometric analysis than other peptides (Fleischer et al 2006).

Proteins that were not present in the control samples and which associated with wild-type PAB1 in 40% or less of the mass spectrometric experiments were less likely PAB1-associated proteins (Table 4). Proteins that were not present in the control samples and which were present in greater than 40% of the experimental samples with Flag-PAB1 were considered to be more likely PAB1-associated proteins. Table 5 lists these 44 proteins, the average number of unique peptides observed in each case, their protein abundance factor (PAF), and the most likely function related to PAB1. A PAF value represents the number of average unique peptides observed divided by the molecular weight of the protein (10 x KDa). The PAF value normalizes the number of unique peptides to the size of the protein, which in turn is proportional to the number of possible tryptic peptides that could be observed in this experiment (Fleischer et al 2006).

We judged that our analysis was detecting and identifying specific PAB1-mRNP contacts by three means. First, the summary of two different TAP mass spec analyses of the yeast proteome (Collins et al 2007; Ho et al 2002; Gavin et al 2002) have identified 41 significant non-ribosomal protein contacts to PAB1. Of the top 12 proteins on this list, we identified eight of these (eIF4G1, eIF4G2, CBC1, NAB6, NAB3, SGN1, GBP2, and CBF5). Other 4 protein do not in our list are FUN12, NPL3, MAG1, and SPT2. FUN12 is a GTPase, required for general translation initiation by promoting Met-tRNA^{iMet} binding to ribosomes and ribosomal subunit joining. NPL3 carries poly(A) mRNA from nucleus to cytoplasm; MAG1 involved in DNA damage repair. SPT2 is required for RNA polyadenylation. To date, SGD (<http://thebiogrid.org/36918>) shows 142 proteins which have been detected as interacting with PAB1. Twelve of these proteins are also in our top list (eIF4G1, eIF4G2, eIF4E, NAB3, NAB6, SBP1, PBP2, SGN1, SUP35, and RRP5, yGR054w, and SMB1). The difference between our results and other researcher's is easy to understand because first, a number of parameters, including cell growth and lysis, immunoprecipitation conditions, digestion efficiency and recovery of peptides from gel slices, and run-to-run variations in mass spectrometry, among others, contribute to this variability. Second, none of these mass spectrometric experiments were conducted by using PAB1 as bait.

Second, PAB1 direct interactions with proteins have been studied by other biochemical procedures. Translation initiation factors eIF4G1 and eIF4G2 are known to contact PAB1 through its domains RRM1 and RRM2 (Tarun and Sachs 1996; Otero et al 1999), eRF3, involved in translation termination, is known to contact PAB1 through its C domain (Gorgoni and Gray 2004), and PBP2 is known to contact PAB1 through either the P or C domain (Mangus et al 1998). All four of these proteins were found in our group of 44 proteins associating with the PAB1-mRNP structure.

Third, our list of 44 proteins contains 38 proteins that would be expected to associate with the PAB1-mRNP complex. There are eight proteins involved in translation, six in mRNA decay, six in RNA binding, four in mRNA transport or binding in the nucleus, and another fifteen proteins in nucleolar and/or ribosomal biogenesis, all processes known to include PAB1 (Table 5). Only seven other proteins were identified that play no obvious roles related to that of PAB1.

Protein	Mol wt (KDa)	Unique peptides (Avg)	PAF score	Function related to PAB1
RPB1	192	2.4	0.12	Transcription
TOP2	164	4.2	0.090	DNA metabolism
SKI2	147	2.2	0.15	mRNA degradation
RMD11	131	2.8	0.21	Unknown
MAK21	117	2.2	0.19	Nucleolar
PWP1	64	0.8	0.12	Nucleolar
AEP1	60	2.6	0.43	Unknown
PRP4	53	0.6	0.11	Splicing
NSR1	27	0.6	0.22	Nucleolar

Table 4, Legend: Average number of unique peptides identified by mass spectrometric analysis across all wild-type PAB1 pull-downs for proteins not present in the control experiments. Proteins in the list were identified in 40% or less of the mass spectrometric experiments.

Protein	Mol wt (KDa)	Unique peptides (Avg)	PAF score	Function related to PAB1
AEP2	68.1	7.4	1.1	Mitochondrial
BRX1	33.7	2.6	0.77	Nucleolar
CBC1	99.7	14	1.4	RNA binding
CBF5	55.2	8.4	1.5	Nucleolar
CLU1	145	9.8	0.68	Translation initiation
eIF4G1	107	31	2.9	Translation initiation
eIF4G2	104	13	1.2	Translation initiation
ENP2	82	2.1	0.26	Nucleolar
eRF3	76.9	12	1.5	Translation
GBP2	49	8.4	1.7	mRNA export
HRB1	49.3	4	0.81	mRNA export
KRI1	68.6	3.6	0.52	Nucleolar
KRR1	37.4	3.8	1	Nucleolar
LHP1	32.2	5.3	1.6	Nucleolar
MIS1	107	12	1.1	Mitochondrial
MNP1	20.6	1.4	0.68	Mitochondrial
NAB3	90.5	2.6	0.29	RNA binding
NAB6	127	11	0.87	RNA binding
NOP6	25.2	3.3	0.13	Nucleolar
NOP77	78.1	7	0.9	Nucleolar
NUG1	57.8	3.8	0.68	Nucleolar
PBP2	45.6	5.7	1.2	RNA binding
PUB1	48	4.6	0.96	RNA binding
RLP7	36.7	2.7	0.74	Nucleolar
RLR1	185	15	0.81	THO complex
RPA190	188	10	0.53	Transcription
RRP12	114	13	1.1	Nucleolar
RRP5	194	50	2.6	Nucleolar
RSE1	155	3.2	0.21	Splicing
SGN1	30	4.6	1.5	RNA binding
SKI3	165	8.6	0.52	mRNA degradation
SLF1	50.9	5	0.98	Translation
SSD1	140	19	1.4	RNA binding
TMA46	46.3	3.2	0.69	Translation
UBP3	102	3	0.29	Nucleolar
UPF1	110	14	1.3	mRNA degradation
URB1	204	2.6	0.13	Nucleolar
UTP20	288	13	0.45	Nucleolar
XRN1	176	40	2.3	mRNA degradation
YEF3	117	6	0.51	Translation
yGR054w	71.8	5.6	0.78	Translation initiation
yGR250c	89.7	7	0.78	Translation
yIL055c	70.8	4	0.56	Unknown
yLR419w	164	10	0.61	RNA helicase

Table 5, legend: lists of 44 likely PAB1-associated proteins.

Stoichiometric association within the PAB1-mRNP was judged by protein abundance factor (PAF). Based on current model, there is expected to be only one copy of eIF4G in each PAB1-mRNP complex. Therefore, those proteins with a PAF value close to that of eIF4G1 or eIF4G2 or higher may present in roughly equal stoichiometry within the PAB1-mRNP complex. Only 21 proteins were found to associate with PAB1 in relatively equivalent levels to that of eIF4G1/2 (Table 6). All of these proteins were predicted to be RNA associated factors of one type or another. Therefore, these 21 proteins that we found associated with PAB1 in near equivalent abundances could be components of the closed-loop structure.

Notably absent from our Flag-PAB1 complexes were eIF1, -2, -3, and -5 components. We did observe that CLU1 (an eIF3 component) and yGR054w (an eIF2 factor) associated specifically with PAB1-mRNP, but they did not appear at all in equivalent amounts to that of eIF4G, as each was 70-fold less abundant. This is reasonable because these factors are known to be transiently associated within the mRNP complex and these initiation factors dissociate from the resulting initiation complex. Decapping and deadenylase complex components were also notably absent from our purified Flag-PAB1 material, indicating that we were not purifying P-bodies (Parker and Sheth 2007).

Protein	MW(Da)	pI	Function
AEP2	67523	10.33	Mitochondrial protein, likely involved in translation of the mitochondrial OLI1 mRNA; exhibits genetic interaction with the OLI1 mRNA 5'-untranslated leader
CBC1	100017	4.64	Large subunit of the nuclear mRNA cap-binding protein complex, interacts with Npl3p to carry nuclear poly(A)+ mRNA to cytoplasm; also involved in nuclear mRNA degradation and telomere maintenance; orthologous to mammalian CBP80
CBF5	54704	9.5	Pseudouridine synthase catalytic subunit of box H/ACA small nucleolar ribonucleoprotein particles (snoRNPs), acts on both large and small rRNAs and on snRNA U2; mutations in human ortholog dyskerin cause the disorder dyskeratosis congenita
GBP2	48728	6.16	Poly(A+) RNA-binding protein, involved in the export of mRNAs from the nucleus to the cytoplasm; similar to Hrb1p and Npl3p; also binds single-stranded telomeric repeat sequence in vitro
KRR1	37159	10.18	Essential nucleolar protein required for the synthesis of 18S rRNA and for the assembly of 40S ribosomal subunit
LHP1	32104	9.02	RNA binding protein required for maturation of tRNA and U6 snRNA precursors; acts as a molecular chaperone for RNAs transcribed by polymerase III; homologous to human La (SS-B) autoantigen
MIS1	106216	9.16	Mitochondrial C1-tetrahydrofolate synthase, involved in interconversion between different oxidation states of tetrahydrofolate (THF); provides activities of formyl-THF synthetase, methenyl-THF cyclohydrolase, and methylene-THF dehydrogenase
NAB3	90438	4.22	Single stranded RNA binding protein; acidic ribonucleoprotein; required for termination of non-poly(A) transcripts and efficient splicing; interacts with Nrd1p
NAB6	126138	6.99	Putative RNA-binding protein that associates with mRNAs encoding cell wall proteins in high-throughput studies; deletion mutants display increased sensitivity to some cell wall disrupting agents; expression negatively regulated by cAMP
NOP12	51941	10.22	Nucleolar protein involved in pre-25S rRNA processing and biogenesis of large 60S ribosomal subunit; contains an RNA recognition motif (RRM); binds to Ebp2; similar to Nop13p and Nsr1p
NOP77	77825	9.81	Nucleolar protein, essential for processing and maturation of 27S pre-rRNA and large ribosomal subunit biogenesis; constituent of 66S pre-ribosomal particles; contains four RNA recognition motifs
PBP1	78781	6.91	Component of glucose deprivation induced stress granules, involved in P-body-dependent granule assembly; similar to human ataxin-2; interacts with PAB1 to regulate mRNA polyadenylation; interacts with Mkt1p to regulate HO translation
PBP2	45782	7.69	RNA binding protein with similarity to mammalian heterogeneous nuclear RNP K protein, involved in the regulation of telomere position effect and telomere length

PUB1	50763	4.81	Poly(A) + RNA-binding protein, abundant mRNP-component protein that binds mRNA and is required for stability of many mRNAs; component of glucose deprivation induced stress granules, involved in P-body-dependent granule assembly
RRP12	137507	7	Protein required for export of the ribosomal subunits; associates with the RNA components of the pre-ribosomes; contains HEAT-repeats
RRP5	193133	6.1	RNA binding protein with preference for single stranded tracts of U's involved in synthesis of both 18S and 5.8S rRNAs; component of both the ribosomal small subunit (SSU) processosome and the 90S preribosome
SBP1	32989	5.45	Putative RNA binding protein; involved in translational repression and found in cytoplasmic P bodies; found associated with small nucleolar RNAs snR10 and snR11
SGN1	28954	10.13	Cytoplasmic RNA-binding protein, contains an RNA recognition motif (RRM); may have a role in mRNA translation, as suggested by genetic interactions with genes encoding proteins involved in translational initiation
SLF1	50943	10.11	RNA binding protein that associates with polysomes; proposed to be involved in regulating mRNA translation; involved in the copper-dependent mineralization of copper sulfide complexes on cell surface in cells cultured in copper salts (1, 2)
SMB1	22379	11.15	Core Sm protein Sm B; part of heteroheptameric complex (with Smd1p, Smd2p, Smd3p, Sme1p, Smx3p, and Smx2p) that is part of the spliceosomal U1, U2, U4, and U5 snRNPs; homolog of human Sm B and Sm B'
SSD1	139953	7.67	Protein with a role in maintenance of cellular integrity, interacts with components of the TOR pathway; <i>ssd1</i> mutant of a clinical <i>S. cerevisiae</i> strain displays elevated virulence
SUP35	76551	7	Translation termination factor eRF3; altered protein conformation creates the [PSI(+)] prion, a dominant cytoplasmically inherited protein aggregate that alters translational fidelity and creates a nonsense suppressor phenotype
UPF1	109429	6.45	ATP-dependent RNA helicase of the SFI superfamily involved in nonsense mediated mRNA decay; required for efficient translation termination at nonsense codons and targeting of NMD substrates to P-bodies; involved in telomere maintenance
XRN1	175458	7.5	Evolutionarily-conserved 5'-3' exonuclease component of cytoplasmic processing (P) bodies involved in mRNA decay; plays a role in microtubule-mediated processes, filamentous growth, ribosomal RNA maturation, and telomere maintenance
yGR250c	89512	5.1	Putative RNA binding protein; localizes to stress granules induced by glucose deprivation; interacts with Rbg1p in a two-hybrid .

Table 6, Legend: List of proteins that were found to associate with PAB1 in relatively equivalent levels to that of eIF4G. pI indicate Isoelectric Point and MW indicate Molecular

Weight. The information on each protein was obtained from the *Saccharomyces* genome database. Also, other papers suggested yGR250c, PBP1, NAB3 was associated with PAB1 and were added in the list.

Because PAB1 has a variety of roles in the cell, these 25 proteins do not necessary have to be all present in the closed-loop structure. They could be associated with PAB1 indirectly or in other PAB1 complexes that have yet to be discovered. To further study these putative proteins and determine if they exist in the translation complex, we used the novel technique of analytical ultracentrifugation with a fluorescent detection system (AU-FDS) to identify translation complexes.

Analytical ultracentrifugation (AUC) identifies a 78S complex and polysomal material in Flag-PAB1 immunoprecipitated material

Crude extracts subjected to AUC analysis (Figure 11) displayed the typical 40S, 60S, 80S and polysomal material observed in the more standard sucrose gradient analysis of mRNP complexes (Figure 12, from Patrick, 1998). This result indicated that we could use AUC to characterize the ribosome profile.

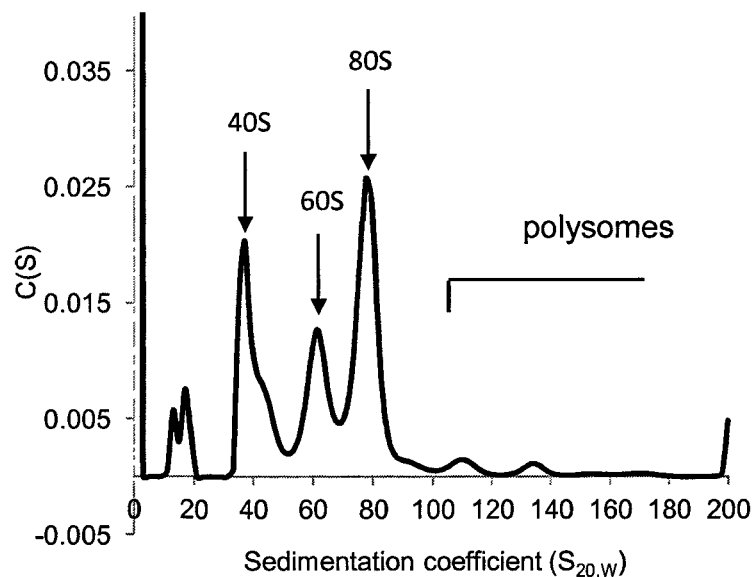


Figure 11, Legend: Cells were grown at 30°C, harvested at an OD600 nm of 0.8. AUC analysis (run speed of 15K) with monitoring at A260 was conducted on yeast crude extracts. S (x-axis) represents sedimentation coefficient. Relative absorbance is given on the y-axis. (Data from Xin Wang)

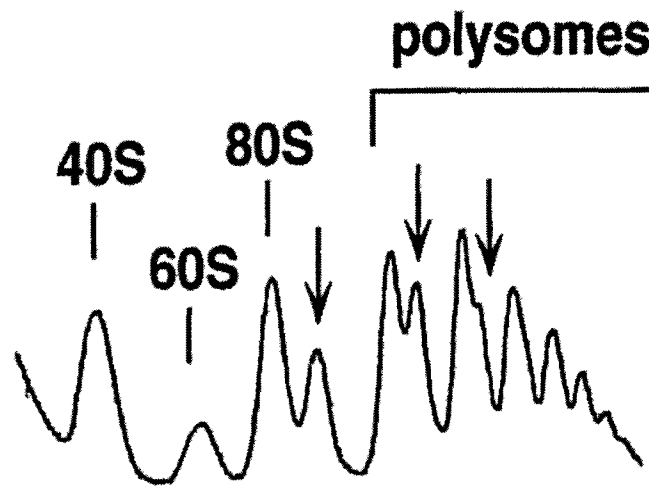


Figure 12, Legend: Cells were grown at 30°C, harvested at an OD_{600 nm} of 0.8, and cell extracts were resolved in 7–50% sucrose gradients. The A_{254 nm} was measured continuously. Sedimentation is from left to right. The peaks of free 40S, 60S ribosomal subunits, 80S ribosome and polysomes are indicated. Half-mers are labelled by vertical arrows. (From Patrick, 1998)

To characterize the sizes of the PAB1 associated complexes that we purified from the strains carrying Flag-PAB1, we subjected the Flag-eluted material to AUC analysis.

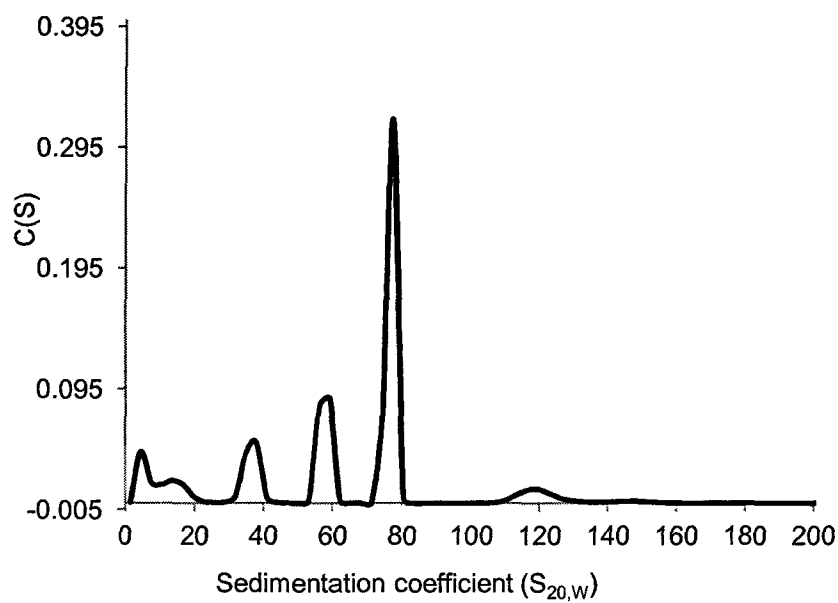


Figure 13, Legend: AUC analysis (run speed of 15K) with monitoring at A260 was conducted on Flag-PAB1 purified material. Sedimentation coefficient ($S_{20,w}$, x-axis) represents sedimentation coefficient. Relative absorbance is given on the y-axis. (Data from Xin Wang)

From AUC analysis, our Flag pull down material showed small peaks less than 20S, 40S, 60S, 78S, and 120S complexes. The signal with greatest intensity was obtained at around 78S.

eIF4E and eIF4G co-migrate with PAB1 in the 78S complex

To determine which of the Flag-PAB1 complexes identified in Figure 11 corresponds to the closed-loop structure, strains carrying Flag-PAB1 and either eIF4E-GFP or eIF4G1-GFP were subjected to Flag pull-down and AU-FDS analysis. eIF4E-GFP, and eIF4G1-GFP were found to migrate in complexes of 78S (Figure 14).

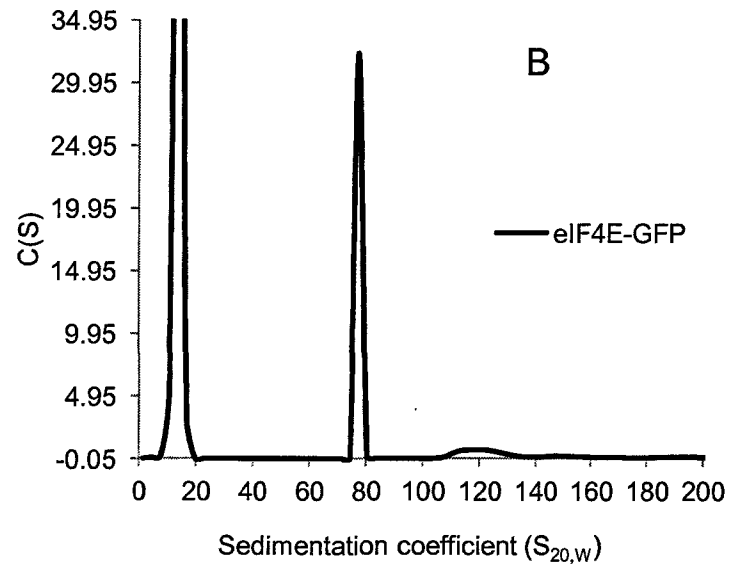
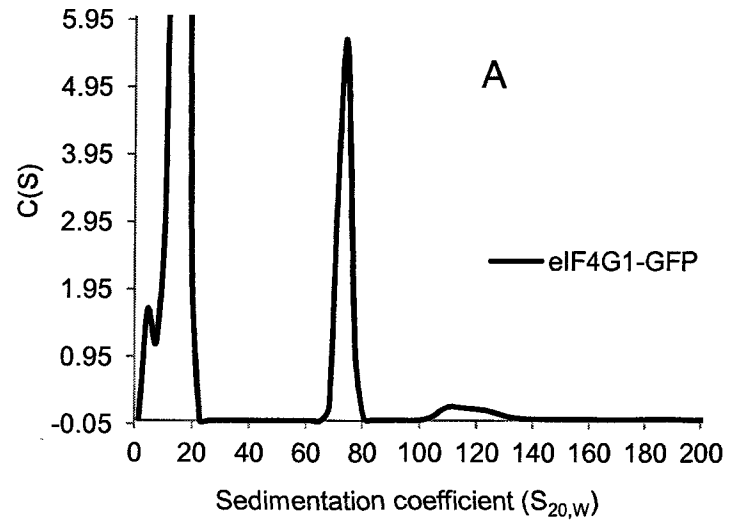


Figure 14, Legend: eIF4G1-GFP (A) and eIF4E-GFP (B) were co-expressed with Flag-PAB1.

Cells were grown at 30°C and harvested at an OD_{600 nm} of ~1.0. AU-FDS was conducted on

Flag pull down material at 15000rpm. (Data from Xin Wang)

It should be noted, however, that the difference in relative intensities for the eIF4E-GFP signal relative to that of eIF4G1-GFP is not due to differences in abundance, as Western analysis on the Flag pull down material identified equivalent levels of the two proteins. For an unknown reason, eIF4E-GFP gives off a fluorescent signal that is much greater than any of the other protein-GFP fusions we have analyzed.

mRNA and ribosomes are present in the 78S Flag-PAB1 complex

To examine which of the Flag-PAB1 complexes carries mRNA, we expressed in yeast along with Flag-PAB1 the U1A RNA binding protein fused to GFP (U1A-GFP) and one mRNA carrying U1A binding sites in the 3' UTR: PGK1p-U1A (Sheth and Parker 2003; Brengues et al 2005). After purification of Flag-PAB1, the resultant complexes were subjected to AU-FDS. As shown in Figure 15, the mRNA migrated in a 78S complex, coincident with eIF4E, eIF4G1, and Flag-PAB1. These data indicate that the mRNA is in the 78S complex.

We also inquired as to whether the 78S complex contained the 40S and 60S ribosomal subunits. The 40S subunit of ribosome has a ~1900 nucleotide (18S) RNA and ~33 proteins. RPS4B is one of the abundant proteins in the 40S subunit. As shown in Figure 15, RPS4B-GFP migrates about 40S and 78S peak following

Flag-PAB1 purification. These data indicate that the small ribosome subunit is in the 78S complex. These data indicate that mRNA, small ribosome subunit and large ribosome subunit present in the 78S peak. This data demonstrate that PAB1, eIF4G, eIF4E, mRNA, and ribosome are all found in the 78S peak, thus this 78S peak from our Flag pull-down material is most likely the 78S ribosome translation initiation complex in a closed-loop structure.

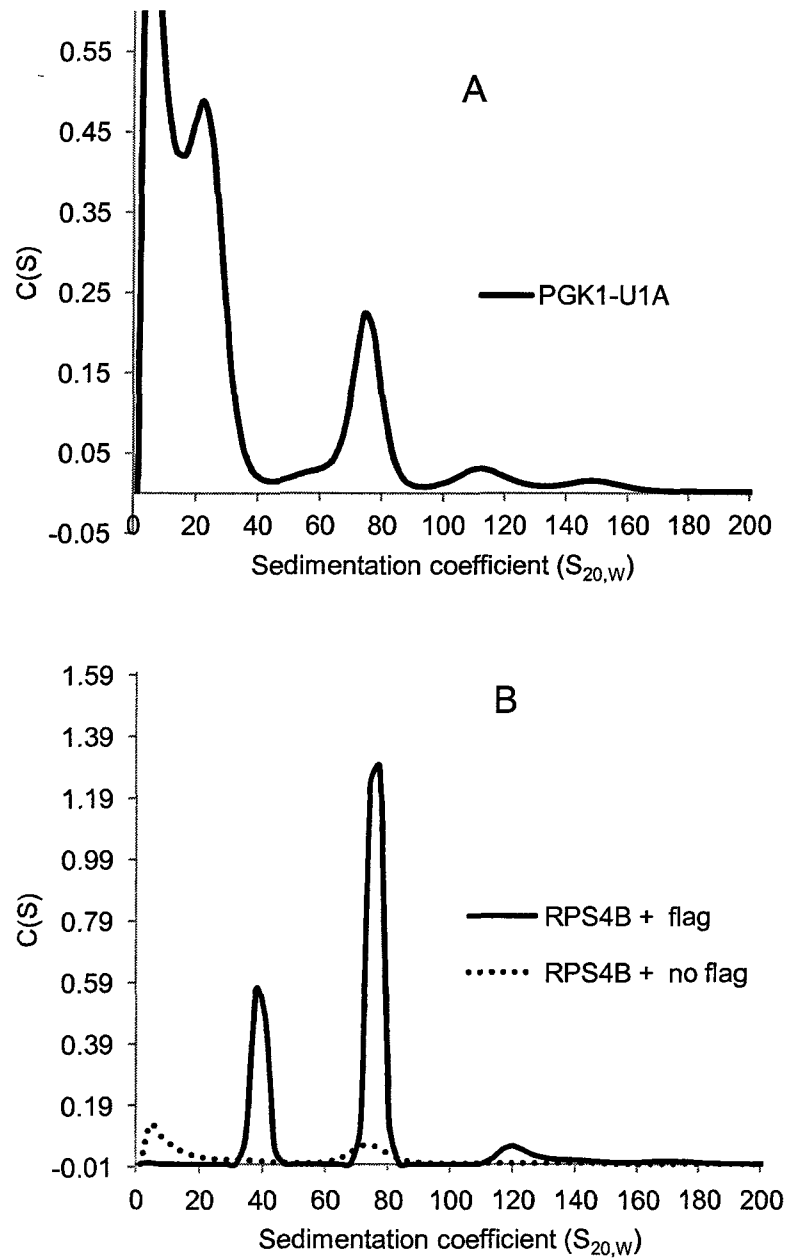
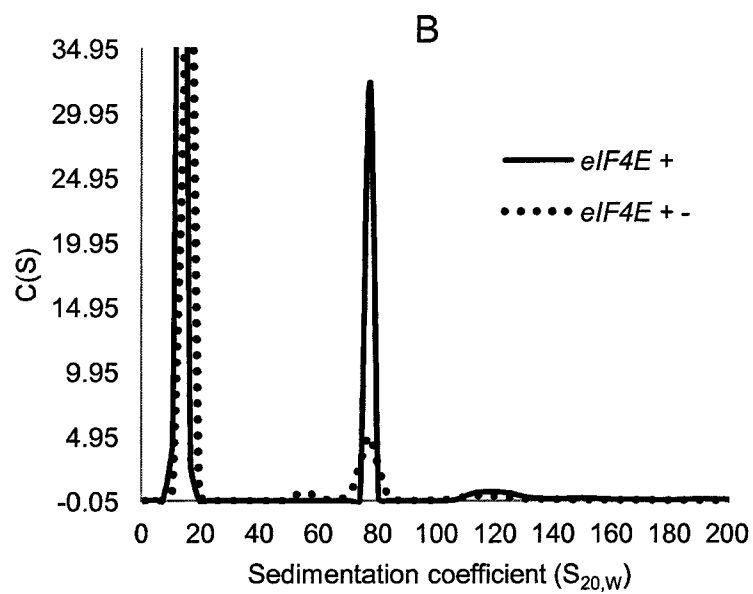
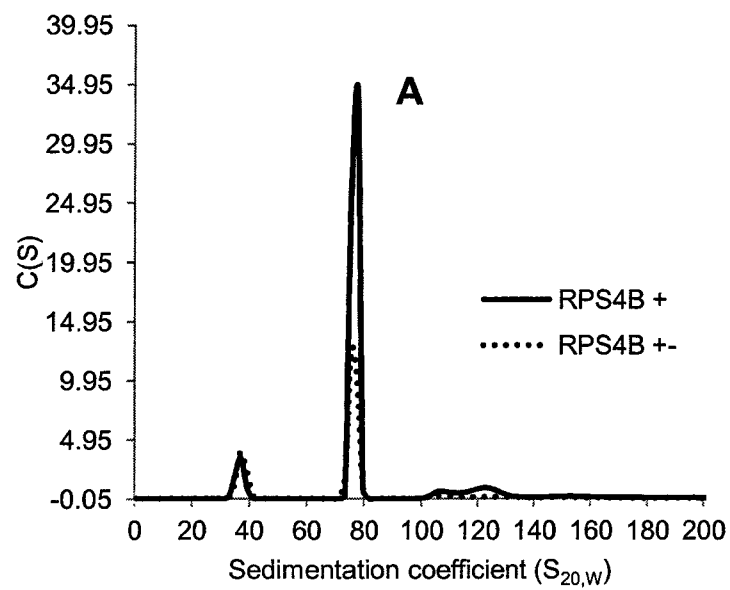


Figure 15, Legend: A, the RNA binding U1A protein fused to GFP (U1A-GFP) and one mRNA carrying U1A binding sites in the 3' UTR was co-expressed with Flag-PAB1. Cells were grown at 30°C and harvested at an OD_{600 nm} of ~1.0. AU-FDS was conducted on Flag pull down material at 15000rpm. B, same as A, except RPS4B-GFP protein was co-expressed with Flag-PAB1 (RPS4B+Flag) or PAB1 without Flag tag (RPS4B no Flag). (B from Xin Wang)

The 78S complex peak is reduced upon the stress of glucose deprivation

We subsequently analyzed the effect of the stress of glucose deprivation upon the formation of the 78S Flag-PAB1 complex, as such a stress is known to block translation (Ashe et al 2000). As shown in Figure 16, stress resulted in much less RPS4B-GFP in the 78S complex. The same results for the effect of glucose deprivation on the 78S complex migration have been found for eIF4E, eIF4G1, mRNA, PAB1, eIF4G2, and RPS4B. Re-addition of glucose to depleted cells reestablishes translation and at the same time we found that presence of these proteins were present the in the 78S complex. These results suggest that the 78S complex corresponds to a translationally competent structure that disappears upon stress-induced translational cessation.



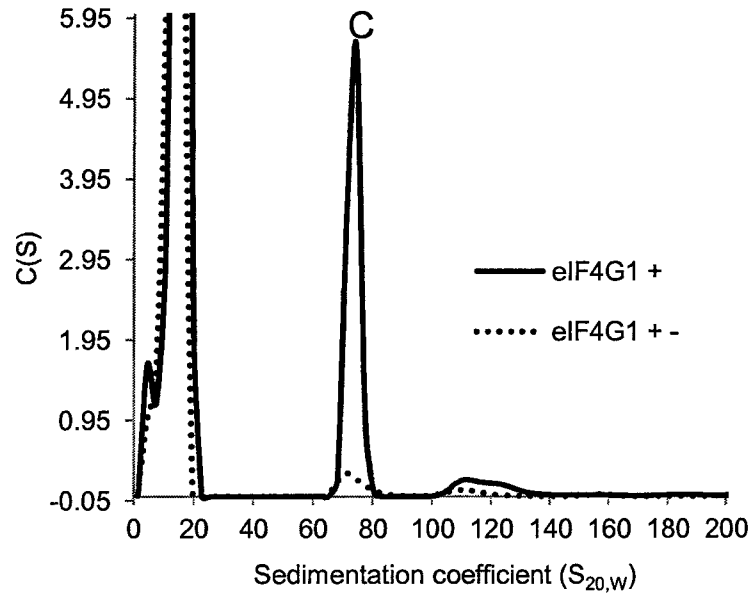
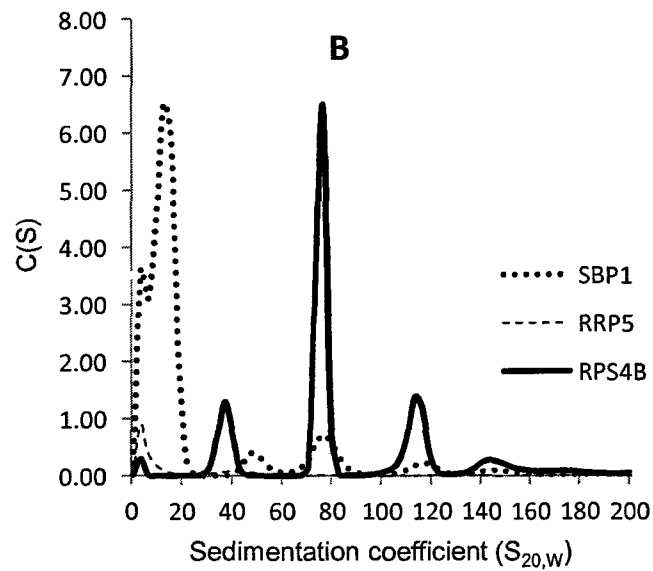
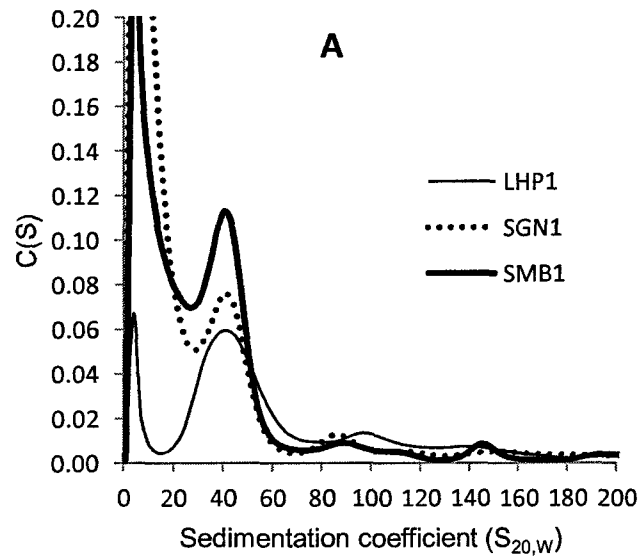


Figure 16, Legend: A, RPS4B-GFP were co-expressed with Flag-PAB1, Cells were grown overnight on glucose-containing medium before splitting into untreated cells (RPS4B+) or cells deprived of glucose for 30 min (RPS4B+-), and AU-FDS was conducted on Flag pull down material at 15000rpm. B and C same as A, except eIF4G-GFP or eIF4E-GFP were co-expressed with Flag-PAB1. (B and C from Xin Wang)

These correlations indicate that we can identify unknown components of the 78S complex by the following simple methodology. First, proteins that have previously been demonstrated to immunoprecipitate with PAB1 will be considered possible candidates of the 78S complex. Second, GFP fusions to these proteins will be co-expressed in yeast with Flag-PAB1. Third, following purification of Flag-PAB1, the size of complexes that the GFP-fusion protein migrates in will be determined by AU-FDS. As a control, Flag immunoprecipitations will be conducted on the strains carrying the GFP fusion protein and PAB1 lacking the Flag tag. Fourth, the migration of such GFP-fusion proteins in a 78S complex will be confirmed by subjecting yeast to glucose depletion prior to isolating the Flag-PAB1 complexes and AU-FDS analysis. Reduced levels of the GFP-fusion in the 78S complex following glucose depletion will suggest that it is a component of this complex. Re-conducting the experiment by adding glucose back to depleted cells for 10 min following glucose depletion will ascertain whether that the association in the 78S complex correlates with the translational state. Western blot analysis will be conducted on all Flag purified material to establish that equivalent levels of material were subjected to AU-FDS analysis: eIF4E as well as Flag-PAB1 levels will be assessed. As some proteins may be less stably associated with the complex than others, as has been demonstrated for TIFs eIF1, 2, 3 and 5, each of our experiments will also be conducted following treatment of the cells with formaldehyde to stabilize the 78S complex. Such treatment has been shown not to affect the formation of the translation complex (Nielsen et al 2007). As AUC

data analysis is a data fit process, it is not surprising the sedimentation coefficients of the 78S translation complex may undergo slight changes from experiment to experiment.

AU-FDS analysis results for 25 putative proteins which associate with PAB1



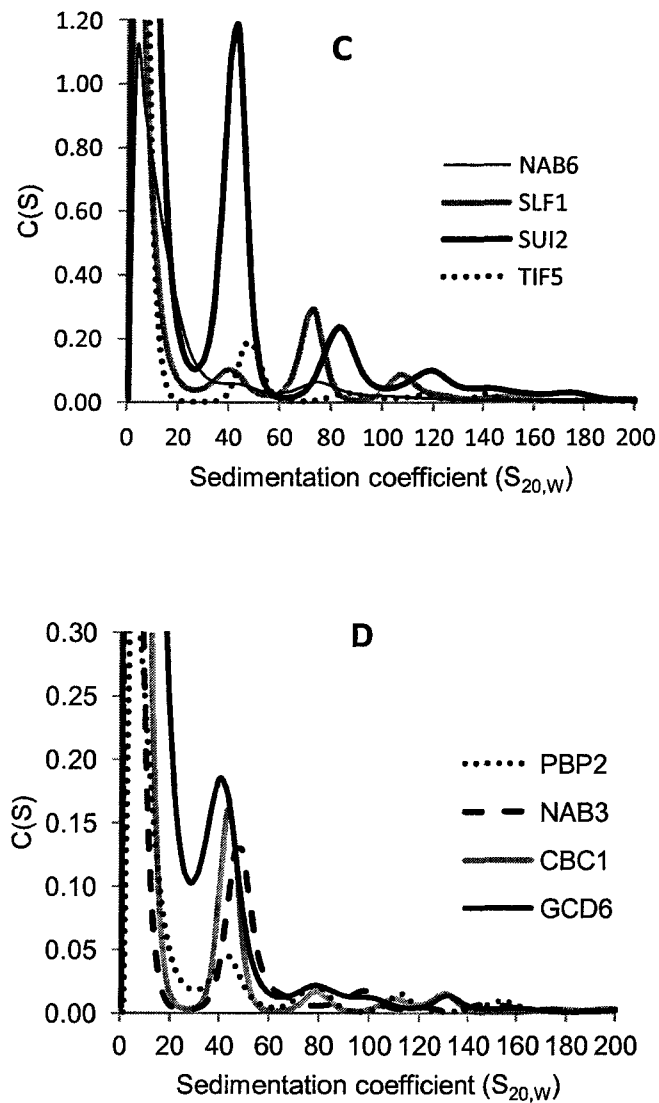


Figure 17, Legend: 14 proteins (Shown in A through D) were fused with GFP and co-expressed with Flag-PAB1 one at a time. Flag purified material were analyzed with AU-FDS. Formaldehyde treatment was used before cell lysis to stabilize the mRNP complex.

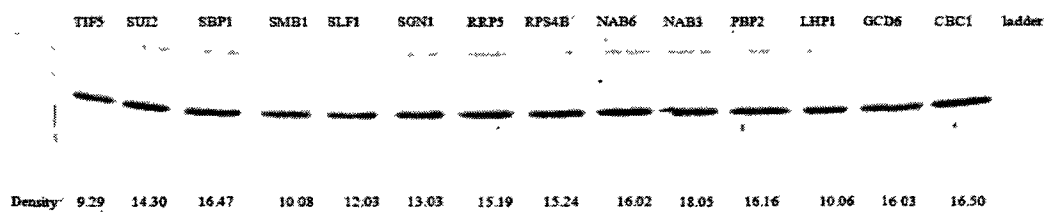
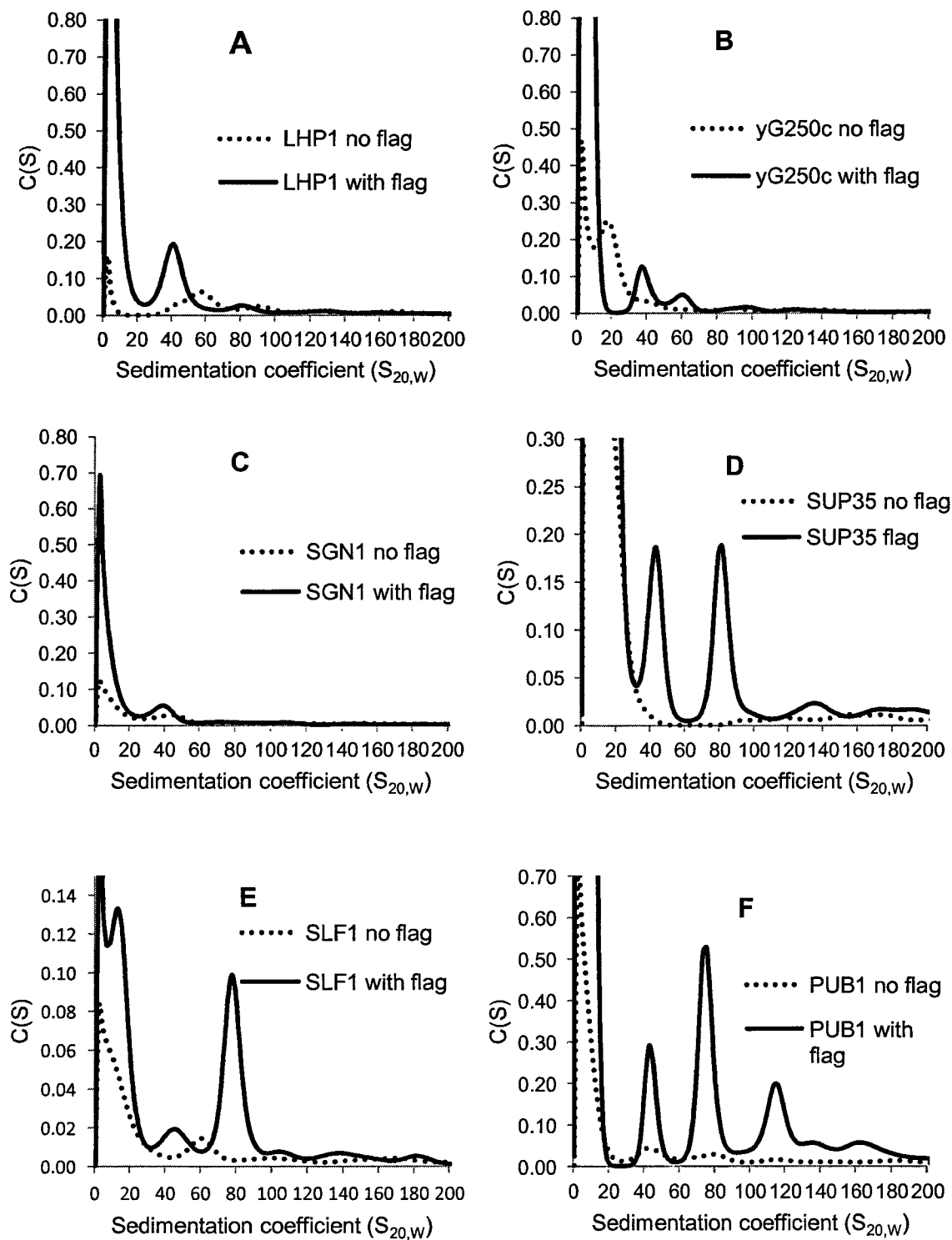


Figure 18, Legend: Western Blot was conducted for each Flag pull down preparation to check the relative amount protein loaded to AU-FDS cell. Antibody against eIF4E was used. After Western analysis, density scans for each band was performed with LI-COR Scanner. The values represent the the relative intensities of the eIF4E protein in each of the preparations.

In order to identify which protein is present in the 78S translation complex, we first screened all 25 proteins by using AU-FDS. Each of these experiments was conducted following treatment of the cells with formaldehyde to stabilize the 78S complex. Strains carrying Flag-PAB1 and corresponding GFP fusion protein were immunoprecipitated on a Flag beads column, eluted with excess Flag peptide, and subjected to AU-FDS analysis. As shown in Figure 17, SBP1 and RPS4B displayed peaks around 40S, a 78S peak with high intensity, and polysomes. RPS4B, a component of 78S complex, was used as control at this time. SUI2, and SLF1 displayed a peak around 40S, a relative high intensity 78S peak (around 0.2) and polysomes; suggesting that SBP1, SUI2 and SLF1 are likely to be present in the 78S complex. LHP1, SGN1, SMB1, RRP5, NAB6, NAB3, TIF5, GCD6, CBC1, and PBP2 displayed a peak around 40S and low intensity peaks in the vicinity of 78S. However, they displayed significantly different signal intensity (intensity around 0.02). Western blot analysis was conducted for each Flag pull-down preparation to establish that roughly equivalent levels of material were subjected to AU-FDS analysis. A typical western blot is shown in Figure 18, in which eIF4E was detected, and Flag-PAB1 was also defined by using anti-Flag antibody (not shown). After Western analysis, eIF4E levels were assessed by density scan with a LI-COR Scanner and displayed no significant difference between preparations. The RPS4B, SBP1, SUI2, and SLF1 displayed relative high intensity in 78S complex in these 14 proteins, while the eIF4E densities of these proteins are 15, 16, 14, and 12 respectively. On the other hand, CBC1,

GCD6, PBP2, NAB3 and NAB6 showed similar relatively high eIF4E densities (around 16), but the intensities of 78S peak corresponding to these proteins were much lower, suggesting that the lower intensity might only represent background level of fluorescence. After screening all of the 25 proteins fused with GFP, we found that all of these proteins contained complexes that migrated at about 78S peak but they all displayed different intensities. Since each experiment was repeated at least twice, only the SBP1, SLF1, PUB1, SSD1, SUP35, SUI2, and PRT1 displayed a 78S peak with a signal intensity greater than 0.1.

Before eliminating the other 18 proteins as not being components of the 78S complex, we determined if the lower intensity signal were above the background signal. We conducted AU-FDS on extract from strains expressing each of these GFP fusions proteins carrying Flag-PAB1 or PAB1 at the same time. The results are shown in Figure 19 for seven proteins we believe are part of the 78S complex, SBP1, SLF1, PUB1, SSD1, SUP35, SUI2, PRT1 and three negative examples of the proteins that had displayed low 78S intensity, LHP1, yGR250c, and SGN1.



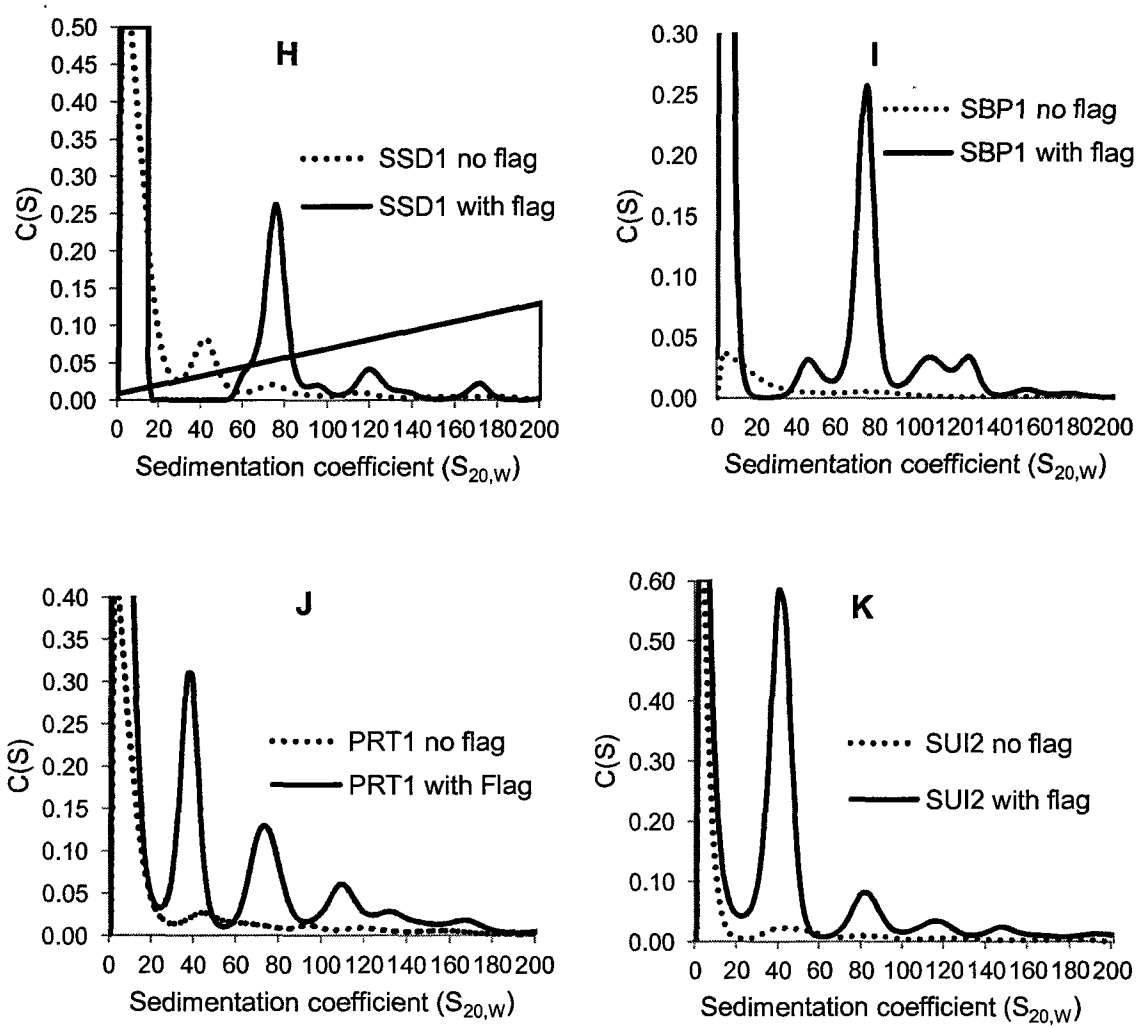


Figure 19, Legend: proteins (Shown in A through K) were fused with GFP and co-expressed with Flag-PAB1 (with Flag) or with PAB1 only (no Flag) one at a time. Flag purified material were analyzed with AU-FDS. Formaldehyde treatment was used before cell lysis to stabilize the mRNP complex.

Figure 19 A, B, and C shows that no 78S complex for LHP1-GFP, yGR250c-GFP, and SGN1-GFP in the Flag-PAB1 immunoprecipitation was significantly distinguished as compared to the controls. Similar to LHP1, yGR250c, and SGN1, the same type of results were found for GFP fusions to HRP1, CBC1, SMB1, PBP1, PBP2, RRP5, RRP12, XRN1, UPF1, GCD1, GCD6, GCD11 and GBP2 (data not shown). These results indicate that these proteins are unlikely to be associated with the 78S translation complex. Because PAB1 plays multiple roles in the cell, our mass spectrometric detection of a number of these proteins suggest that we could possibly be pulling down other PAB1 associated complexes; For example, all of these proteins displayed a peak around 40S, suggesting that these proteins may be present in a complex around 40S. However, the character of this complex is still unclear.

Figure 19 D through K shows a clear 78S complex for GFP fusions to SUP35, SBP1, SLF1, SSD1, PUB1, PRT1 and SUI2. This set of proteins showed a relatively high signal in the 78S peak relative to a very low signal when a strain carrying PAB1 and the corresponding GFP fusion proteins were purified on Flag beads column and subjected to AU-FDS analysis. These results suggested these proteins were most likely in the 78S translation complex. Interestingly, all of these protein also showed a peak around 40S, especially for SUI2 and PRT1 which displayed a higher intensity peak around 40S than that of 78S peak. SUI2 is the alpha subunit of the translation initiation factor eIF2; PRT1 is the eIF3b subunit of the core complex of translation initiation factor 3. They are known to be removed

from the complex when the 60S ribosome subunit join to the 48S preinitiation complex. Formaldehyde treatment appeared to stabilize the association of SUI2 and PRT1 within 78S translation complex. Without formaldehyde treatment, we could not detect SUI2-GFP and PRT1-GFP in the 78S complex (Figure 20).

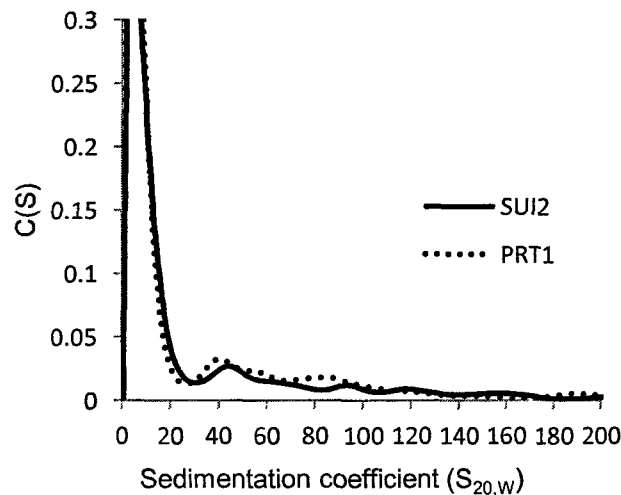
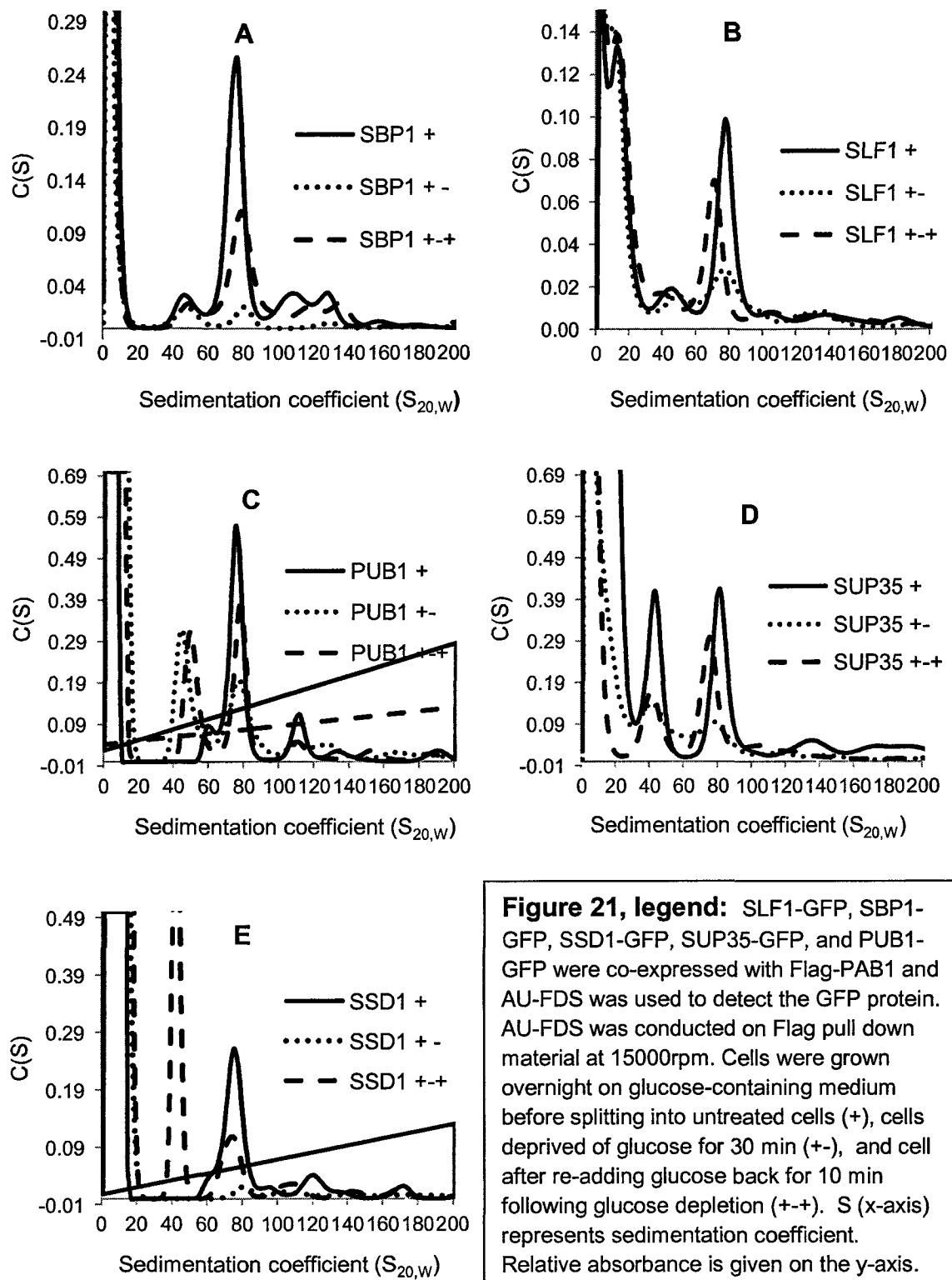


Figure 20, legend: SUI2 and PRT1 protein were fused with GFP and co-expressed with Flag-PAB1. Flag purified material were analyzed with AU-FDS, without formaldehyde treatment before cell lysis.

To eliminate possible side effect of formaldehyde, we conducted AU-FDS analysis for SBP1, SLF1, SUP35, SSD1, and PUB1 without formaldehyde. As shown in Figure 21, all of these proteins displayed significant 78S complex. Because SBP1, SLF1, SUP35, SSD1 and PUB1 are likely to be components of the 78S complex, we wished to verify this by testing whether their presence in the 78S complex was affected by the stress of glucose depletion. As indicated above, if they disappeared from the 78S complex upon glucose depletion and

translation stoppage, as did the 78S complex, then we would conclude that these proteins are present in the 78S complex. The glucose depletion treatment and re-addition of glucose were performed to ensure that a reduced signal obtained with glucose depletion could be re-obtained after glucose was added back. The results are shown in Figure 21. Western blots conducted on all samples to ensure that the Flag pull down process was equally successful. Flag-PAB1 levels were assessed (Figure 21).



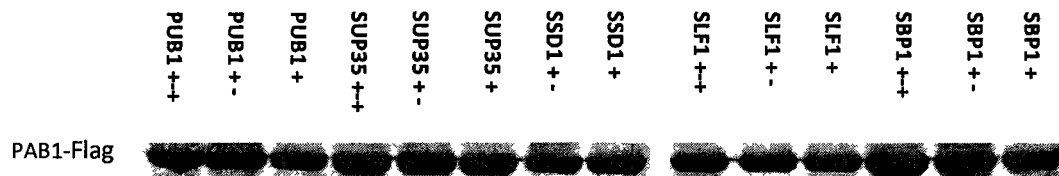


Figure 22, legend: Western Blots were conducted for each Co-IP preparation to check the relative amount protein loaded to AU-FDS cell. Proteins fused with GFP were co-expressed with PAB1-Flag. Cells were grown overnight on glucose-containing medium before splitting into untreated cells (+), cells deprived of glucose for 30 min (+-), and re-adding glucose back to depleted cells for 10 min following glucose depletion (+-+).

	1	2	3	4	average	SEM
SBP1	4.1	9.3	11.2	12.2	9.2	1.8
SLF1	4.3	6.3	10.2		6.9	1.7
SUP35	4.8	3.9			4.4	0.4
SSD1	12.0	13.0			12.5	0.5
PUB1	3.0	3.5			3.3	0.3

Table 8, Legend: The 78S complex intensity reduction of glucose depletion compared to normal growth conditions for SBP1, SLF1, SUP35, SSD1, PUB1 in different experiments.

	1	2	3	4	5	6	average	SEM
SBP1	75.6	75.5	75.6	77.6	79.6	75.6	76.6	0.7
SLF1	79.6	77.6	73.5	75.6	73.5	75.6	75.9	1.0
SSD1	73.5	87.6	81.6	75.6	77.6	75.5	78.6	2.1
PUB1	81.6	75.5	73.5	75.6	75.6	77.6	76.6	1.1
SUP35	71.5	75.6	75.6	75.6	71.5	79.9	75.0	1.2

Table 9, Legend: S values for SBP1, SLF1, SSD1, PUB1, and SUP35 in 6 experiments.

As shown in Figure 21, each of these five proteins became similarly depleted from the 78S complex upon glucose depletion. The average reduction (Table 8) was 9.2 ± 1.8 fold for SBP1 in the 78S complex following glucose depletion (four experiments). The signal of SBP1 in the 40S peak displayed no effect in response to glucose depletion but the polysomes were reduced. SLF1 was reduced 6.9 ± 1.7 fold in the 78S peak (three experiments). The signals of SLF1 in the 40S peak and polysomes showed almost no change. The average reduction was 4.4 ± 0.4 fold for SUP35 (two experiments), and the signal of SUP35 in polysomes was also reduced. SSD1 was reduced 12.5 ± 0.5 fold in the 78S peak (two experiments); with almost no effect on polysomes but an increased signal in 40S peak. Finally, PUB1 was reduced 3.3 ± 0.3 fold in 78S peak. SSD1 showed the most difference in this group. Although the 78S complex containing SUP35 and PUB1 showed less difference following glucose depletion, the complex did significantly decrease from glucose to no glucose conditions. Re-addition of glucose to depleted cells reestablishes translation (Ashe et al 2000) and at the same time presence of these proteins in the 78S complex. The western blot results (Figure 22) showed that equivalent levels of PAB1 were subjected to AU-FDS analysis for glucose compare to no glucose conditions. The actual sedimentation coefficients of SBP1-GFP, SLF1-GFP, SSD1-GFP, SUP35-GFP and PUB1-GFP in translation mRNP complex were shown in Table 9. The average sedimentation coefficient for these five proteins was $\sim 77S$, establishing that these five proteins are in the 78S complex. The total of these results suggest

we successfully identified five new proteins (SBP1, SLF1, PUB1, SSD1, and SUP35) involved in the 78S translation complex.

DISCUSSION

Mass spectrometric analysis identified novel proteins in Flag-PAB1 co-immunoprecipitation material.

We successfully purified one or more complexes by using Flag tagged PAB1 immunoprecipitation (Figure 10). In order to define protein components in Flag-PAB1 co-immunoprecipitated complexes, mass spectrometric analysis experiments were conducted. Previous mass spectroscopic experiments reported 142 PAB1 interactors (SGD database). PAB1 is known to play multiple roles, which include mRNA splicing, 3' UTR trimming, transport, translation, and mRNA turnover, suggesting that it could directly or indirectly contact many proteins. However, none of the previous mass spectrometric experiments used PAB1 as bait. Two types of control experiments (done at least in duplicate) were conducted, therefore, in our experiments to eliminate contaminating proteins from the list of proteins interacting with PAB1. This would allow us to identify only those proteins that associated with PAB1 within the context of the PAB1-mRNP structure. We also conducted seven independent Flag-PAB1 immunoprecipitation and mass spectrometric analysis. All proteins identified in the

control experiments were eliminated. Proteins identified in less than 50% of the replicates (3 analyses) were less likely to be present in the initiation complex. Our mass spectrometric analysis identified 44 non-ribosomal proteins as possibly

interacting with PAB1. Relative protein abundances in each experiment were expressed as the total number of nonredundant tandem mass spectra that correlated significantly to each ORF normalized to the molecular weight of the cognate protein ($\times 10^4$). Twenty one of these were considered to more likely exist alongside PAB1 in the translation initiation complex. The difference between our results and other researchers' is easy to understand because a number of parameters, including cell growth and lysis, immunoprecipitation conditions, digestion efficiency and recovery of peptides from gel slices, run-to-run variations in mass spectrometry, among others, can contribute to variability.

AU-FDS can be used to identify proteins within the 78S translation complex.

In order to determine which PAB1-containing protein complexes were actually present in our Flag-PAB1 purified material, we subjected the Flag-eluted material to AUC analysis. The previous work in our laboratory showed that in addition to polysomes, the most prevalent complex migrated at 78S. This was based on the fact that extracts from strains carrying Flag-PAB1 and either eIF4E-GFP or eIF4G1-GFP and subjected to Flag-pull-down and AU-FDS analysis, showed that eIF4E-GFP and eIF4G1-GFP1 were found to migrate in complexes of about 78S (73S-80S). It should be noted in regard to the above mentioned variation in S values between individual analyses of a specific complex that this is due in large part to variation in determining the exact meniscus position for AUC analysis.

The mRNA carrying U1A binding sites in their 3' UTR was also co-expressed in yeast with Flag-PAB1 and RNA binding U1A protein fused to GFP and was found to migrate in 78S complex following AU-FDS analysis. The same results were found for RPS4B and RPL6B, small and large ribosomal components, respectively, indicating that the 80S ribosome is also present in the 78S complex. These data from our laboratory indicated that the 78S complex consisted of all the closed loop structural components, eIF4E, eIF4G, PAB1, mRNA, and 80S ribosome. This complex most likely represents an 80S ribosome bound to mRNA in the closed loop configuration. Because an 80S ribosome binds to an mRNA asymmetrically, its predicted size of 98S would not be detected because of increased friction that slow its sedimentation and thereby reduce the sedimentation coefficient.

Furthermore, our laboratory analyzed the effect of the stress of glucose deprivation upon the formation of the 78S Flag-PAB1 complex, as such a stress blocks translation. Glucose depletion resulted in much less eIF4E-GFP and eIF4G1-GFP in the 78S complex. Concomitantly, the MFA2-U1A mRNA presence in the 78S complex was reduced by at least two-fold. These results suggest that the 78S complex corresponds to a translationally competent structure that disappears upon stress-induced translational cessation. To determine whether mRNA that has been translationally silenced by glucose

deprivation can reenter the 78S complex upon the re-addition of glucose, yeast depleted of glucose for 30 minutes and then having glucose added back for 10 minutes prior to isolation of our Flag-PAB1 complexes, showed that after glucose depletion, re-addition of glucose caused eIF4E, eIF4G, RPS4B, RPL6B, and mRNA to reenter the 78S complex coincident with the known re-commencement of translation upon re-addition of glucose (Xin Wang). Hence, the 78S complex is consistent with a translation initiation complex.

These correlations indicate that we could identify unknown components of the 78S complex by the following simple methodology. First, proteins that have previously been demonstrated to immunoprecipitate with PAB1 will be considered possible candidates of the 78S complex. Second, GFP fusions to these proteins will be co-expressed in yeast with Flag-PAB1. Third, following purification of Flag-PAB1, the size of complexes that the GFP-fusion protein migrates in will be determined by AU-FDS. As a control, Flag immunoprecipitations will be conducted on the strains carrying the GFP fusion protein and PAB1 lacking the Flag tag. Fourth, the migration of such GFP-fusion proteins in a 78S complex will be confirmed by subjecting yeast to glucose depletion prior to isolating the Flag-PAB1 complexes and AU-FDS analysis. Reduced levels of the GFP-fusion in the 78S complex following glucose depletion will suggest that it is a component of this complex. Re-conducting the experiment by adding glucose back to depleted cells for 10 mi following glucose depletion will determine that the association in the 78S complex correlates with the

translational state. By this means we would be able to test which of the many proteins we have found to be associated with Flag-PAB1 by mass spectromeric analysis actually were components of the 78S translation complex.

SBP1, SLF1, PUB1, SUP35, and SSD1 are components of the 78S translation complex.

We have successfully been able to demonstrate migration of SBP1-GFP, SLF1-GFP, PUB1-GFP, SUP35-GFP, and SSD1-GFP in the 78S initiation complex by using AU-FDS. Importantly, the presence of these components in the 78S translation complex become significantly reduced following glucose depletion. Re-conducting the experiment by adding glucose back to depleted cells for 10 minutes following glucose depletion showed increased signals for SBP1-GFP, SLF1-GFP, PUB1-GFP, SUP35-GFP, and SSD1-GFP in the 78S complex. Also, confirming that these proteins are part of the 78S complex were our control experiments that demonstrated that Flag immunoprecipitation of extracts from strains carrying only PAB1 and GFP tagged proteins resulted in little or no 78S complex being indentified.

Each of these five proteins may play special roles in the 78S translation complex. SBP1 (formerly known as SSB1), an abundant RNA binding protein, has been

identified as a high-copy-number suppressor of a conditional allele in the decapping enzyme (SGD database). SBP1 protein overexpression restores normal decay rates in decapping-defective strains and increases P-body size and number (Segal et al 2006). In addition, SBP1 protein promotes translational repression of mRNA during glucose deprivation. Moreover, P-body formation is reduced in strains lacking SBP1 protein (Segal et al 2006). Models explaining SBP1 function suggest that SBP1 protein could directly bind mRNA and inhibit the function of translation initiation factors, or SBP1 protein could directly bind the mRNA and facilitates the full assembly of the translational repression complex.

We are the first to report SBP1 protein present in the translation initiation complex, and we think it may play its role in translation initiation. What the function of SBP1 in translation regulation is still not known.

SLF1 is reported as a RNA binding protein that associates with polyribosomes (Sobel et al 1999). It is also involved in the copper-dependent mineralization of copper sulfide complexes on cell surface in cells cultured in copper salts (Yu W et al 1996). Krogan using whole genome mass spectrometric analysis reported SLF1 as interacting with eIF4E (Krogan NJ et al 2006), which is consistent with our results.

Poly (U) binding protein 1 (PUB1) is a cytoplasmic mRNA binding protein that stabilizes transcripts containing AU-rich elements (AREs) or stabilizer elements (STEs). Nuclear poly(A) binding protein 2 (Nab2) interacted with PUB1, and Nab2 functions together with PUB1 to modulate mRNA stability. These data suggest a model where nuclear events are coupled to the control of mRNA turnover in the cytoplasm (Apponi et al 2007). Several lines of evidence also suggest that PUB1 may be involved in mRNA metabolism. Both mammalian homologues of PUB1, HuR and the TIA-1/TIAR, are involved in translational regulation. While HuR acts as a translational enhancer or repressor (López et al 2005), the TIA-1 and TIAR proteins are involved in ARE-mediated translational repression (Piecyk M et al 2000). Radharani et al have examined global mRNA turnover in isogenic *PUB1* and *pub1Δ* strains through gene expression analysis and demonstrate that 573 genes exhibit a significant reduction in half-life in a *pub1Δ* strain. They examined the binding specificity of PUB1 using affinity purification followed by microarray analysis to comprehensively distinguish between direct and indirect targets and found that PUB1 significantly binds to 368 cellular transcripts. PUB1 was found to bind to discrete subsets of cellular transcripts and post transcriptionally regulates their expression at multiple levels (Duttagupta et al 2005). Our demonstration that PUB1 is found in the 78S complex is consistent with PUB1 binding to translating mRNA and therefore being part of the 78S complex. Whether this implies that PUB1 is only surround in the 78S complex because mRNA are also in the complex or plays a functional

role in the 78S complex is unclear. If PUB1 is adventitiously present in the 78S complex because of its binding to so many mRNA, it would be suggest that many other mRNA binding proteins should also be present in the 78S complex. This could be tested by our AU-FDS system.

SUP35 is translation termination factor eRF3. Eukaryotic translation termination is mediated by two interacting release factors, eRF1 and eRF3, which act cooperatively to ensure efficient stop codon recognition and fast polypeptide release. eRF1 recognizes the stop codon in the A site of the ribosome and promotes nascent peptide chain release, and the GTPase eRF3 facilitates this peptide release via its interaction with eRF1 (Zhouravleva et al 1995). In addition to its role in termination, eRF3 is involved in normal and nonsense-mediated mRNA decay through its association with cytoplasmic poly(A)-binding protein (PABP) via PAM2-1 and PAM2-2 motifs in the N-terminal domain of eRF3 (Uchida N et al 2002). SUP35 and PABP interacts with the 3'-poly(A) tail of mRNAs, suggesting that eRF3 may also play an important role in the degradation of mRNAs and/or the regulation of translation efficiency mediated through initiation factors (Amrani N et al 2008). Our demonstration that SUP35 is in the 78S complex suggests that at a very early step of translation SUP35 becomes involved in the process.

SSD1 is a protein with a role in maintenance of cellular integrity and interacts with components of the TOR pathway. Systematic global screens have identified ~200 genes that show genetic or physical interactions with SSD1 (Reguly et al 2006). These genes show a striking enrichment (Hogan et al 2008) for posttranslational modifiers ($p = 10^{-14}$), including 19 kinases and nine histone deacetylases, and genes involved in the cell cycle and cell morphogenesis ($p = 10^{-8}$). SSD1 mutants display sensitivity to high osmolarity, caffeine, fungicides and numerous other compounds, which suggests a role for this protein in the maintenance of cell wall integrity (Ibeas et al 2001), but its mechanism of action remains obscure. In budding yeast, the conserved Ndr/warts kinase Cbk1 localizes to the new daughter cell, where it acts as a cell fate determinant. SSD1 associates with specific mRNAs, a significant number of which encode cell wall remodeling proteins (Hogan et al 2008). Translation of these messages is rapidly and specifically suppressed when Cbk1 is inhibited. This suppression requires SSD1 (Jansen et al 2009). Also, CLN2 is a G1 cyclin involved in regulation of the cell cycle; SSD1 binds to the 5'-UTR of CLN2 mRNA and stabilize it (Ohyama et al 2010). SSD1 may, therefore, like PUB1 be present in the 78S complex because it binds a number of mRNA.

All these five proteins are RNA binding proteins, and evidence showed they are all involved in translational control. We are the first to report that SBP1, SLF1,

PUB1, SUP35 and SSD1 are present in the 78S translation complex. Based on our data, these proteins display much less intensity in the 78S peak compared to eIF4G1, suggesting that these proteins are possibly present in only a subset of mRNP complexes. This result is consistent with PUB1 and SSD1 binding only a subset of mRNA that is present in the 78S complex. Alternatively, these proteins may transiently be present in the 78S complex. The functions of these proteins in translation initiation and regulation yet remain obscure. The significance of this project is that we expand the number of factors present in the 78S translation complex and open a door for studying these proteins' role in translational regulation.

In addition to the above five proteins, we have ruled out CBC1, GCD11, GCD6, GBP2, NAB3, NAB6, PBP1, PBP2, LHP1, RRP12, RRP5, SGN1, SMB1, UPF1, HRP1, XRN1, and yGR250c as being in the 78S translation complex. While these proteins are known RNA binding proteins, the possibility is that they actually are not involved in the 78S translation complex or they do associate with only relatively small numbers of special mRNP complexes. The AUC system may not be able to detect such low concentrations. All these proteins showed a peak around 40S and what the 40S complex is still unclear. The RPS4B-GFP protein was also found to routinely migrate in a ~40S complex as did mRNA. One possibility is that the 40S peak is a degradation product from the 78S complex;

these proteins could randomly bind to partially digested RNA during Flag pull down process because they are all RNA binding proteins. Alternatively, the 40S complex may represent a 40S mRNA-PAB1 complex of novel function. Since eIF4E and eIF4G and the 60S ribosome subunit RPL6B are not significantly part of this complex, it would be a complex that may be a precursor to recruitment of eIF4E or a real mRNA intermediate following translation.

SUMMARY

The major objective of this study was to explore the new components in 78S translation complex.

First, we purified the closed-loop structure using Flag-PAB1. Efficient translation initiation and optimal stability of most eukaryotic mRNAs depends on the formation of a closed loop structure. eIF4E, eIF4G and PAB1 interaction supports the notion of a closed loop mRNP. By using a PAB1 tagged at its N-terminus with the Flag peptide, we could successfully pull out the complex from crude extracts. Our results showed that the 78S translation complex exist in our Flag pull down material, which include the core components (eIF4G, eIF4E, PAB1, mRNA, and 80S ribosome) and other proteins include SBP1, SLF1, SSD1, SUP35, and PUB1.

Second, mass spectrometric analysis detected new proteins possibly exist in the translation initiation complex. Our analyses differ from previous mass spectroscopic data related to PAB1 in that none of these experiments used PAB1 as a bait. Two types of control experiments (done at least in duplicate) were conducted to eliminate contaminating proteins from the list of proteins interacting with PAB1, allowing us to identify only those proteins that associated with PAB1

within the context of the PAB1-mRNP structure. Our mass spectrometric analysis identified 44 non-ribosomal proteins and 21 of which were thought more likely exist in the translation initiation complex.

Third, we developed a new method to identify new components in 78S translation complex. The co-migration of PAB1, eIF4G, eIF4E, mRNA, 40S ribosome subunit, and the 60S large ribosome subunit in a 78S complex and their response to stress condition indicate that we can identify unknown components of the 78S complex by the following simple methodology. First, GFP fusions to possible candidates will be co-expressed in yeast with Flag-PAB1. Second, following purification of Flag-PAB1, the size of complexes that the GFP-fusion protein migrates in will be determined by AU-FDS. As a control, Flag immunoprecipitations will be conducted on the strains carrying the GFP fusion protein and PAB1 lacking the Flag tag. Third, the migration of such GFP-fusion proteins in a 78S complex will be confirmed by subjecting yeast to glucose depletion prior to isolating the Flag-PAB1 complexes and AU-FDS analysis. Reduced levels of the GFP-fusion in the 78S complex following glucose depletion will suggest that it is a component of this complex. Re-conducting the experiment by adding glucose back to depleted cells for 10 min following glucose depletion will determine that the association in the 78S complex correlates with the translational state.

Following the method described above, we identified SBP1, SLF1, SSD1, SUP35, and PUB1 as components of the 78S translation complex. SBP1 is known to be involved in translational repression and SUP35 is a translation termination factor. It is surprising that these two proteins already exist in the translation complex in the initiation step, indicating that these two proteins may play a role in translation initiation and also function as targets for translation termination and response to stress condition. SLF1 is known to interact with eIF4E; PUB1 and SSD1 are involved in the control of at least hundreds of mRNAs. SLF1, PUB1, and SSD1, therefore, seem to be reasonable components of the translation initiation complex. Our data suggest that all of these five new components are involved in translation initiation with the known components for example eIF4E, eIF4G, and PAB1. However, how do SBP1, SLF1, SSD1, SUP35 and PUB1 function in translation initiation remains unknown. In addition, we have ruled out that GBP2, NAB3, NAB6, LHP1, SGN1, SMB1, UPF1, HRP1, XRN1, and yGR250c are in the 78S translation complex.

Alan G. Hinnebusch. eIF3: a versatile scaffold for translation initiation complexes. *Trends Biochem Sci.* 2006 Oct; 31(10):553-62.

Algire MA, Maag D, Savio P, Acker MG, Tarun SZ Jr, Sachs AB, Asano K, Nielsen KH, Olsen DS, Phan L, Hinnebusch AG, Lorsch JR. Development and characterization of a reconstituted yeast translation initiation system. *RNA.* 2002 Mar; 8(3):382-97.

Amrani N, Ghosh S, Mangus DA, Jacobson A. Translation factors promote the formation of two states of the closed-loop mRNP. *Nature.* 2008 Jun 26; 453(7199):1276-80.

Amrani N, Ghosh S, Mangus DA, Jacobson A. Translation factors promote the formation of two states of the closed-loop mRNP. *Nature.* 2008 Jun 26; 453(7199):1276-80.

Anderson JS, Parker RP. The 3' to 5' degradation of yeast mRNAs is a general mechanism for mRNA turnover that requires the SKI2 DEVH box protein and 3' to 5' exonucleases of the exosome complex. *EMBO J.* 1998 Mar 2; 17(5):1497-506.

Anderson P, Kedersha N. RNA granules. *J Cell Biol.* 2006 Mar 13; 172(6):803-8.

Apponi LH, Kelly SM, Harreman MT, Lehner AN, Corbett AH, Valentini SR. An interaction between two RNA binding proteins, Nab2 and Pub1, links mRNA processing/export and mRNA stability. *Mol Cell Biol.* 2007 Sep; 27(18):6569-79.

Asano K, Clayton J, Shalev A, Hinnebusch AG. A multifactor complex of eukaryotic initiation factors, eIF1, eIF2, eIF3, eIF5, and initiator tRNA(Met) is an important translation initiation intermediate in vivo. *Genes Dev.* 2000 Oct 1; 14(19):2534-46.

Asano K, Phan L, Anderson J, Hinnebusch AG. Complex formation by all five homologues of mammalian translation initiation factor 3 subunits from yeast *Saccharomyces cerevisiae*. *J Biol Chem.* 1998 Jul 17; 273(29):18573-85.

Ashe MP, De Long SK, Sachs AB. Glucose depletion rapidly inhibits translation initiation in yeast. *Mol Biol Cell.* 2000 Mar; 11(3):833-48.

Blencowe BJ. Exonic splicing enhancers: mechanism of action, diversity and role in human genetic diseases. *Trends Biochem Sci.* 2000 Mar; 25(3):106-10.

Bonnerot C, Boeck R, Lapeyre B. The two proteins Pat1p (Mrt1p) and Spb8p interact in vivo, are required for mRNA decay, and are functionally linked to Pab1p. *Mol Cell Biol.* 2000 Aug; 20(16):5939-46.

Bouveret E, Rigaut G, Shevchenko A, Wilm M, Seraphin B. A Sm-like protein complex that participates in mRNA degradation. *EMBO J.* 2000 Apr 3; 19(7):1661-71.

Bregues M, Teixeira D, Parker R. Movement of eukaryotic mRNAs between polysomes and cytoplasmic processing bodies. *Science.* 2005 Oct 21; 310(5747):486-9.

Buchan JR, Muhlrads D, Parker R. P bodies promote stress granule assembly in *Saccharomyces cerevisiae*. *J Cell Biol.* 2008 Nov 3; 183(3):441-55.

Burd CG, Matunis EL, Dreyfuss G. The multiple RNA-binding domains of the mRNA poly (A)-binding protein have different RNA-binding activities. *Mol Cell Biol.* 1991 Jul; 11(7):3419-24.

Chen J, Chiang YC, Denis CL. CCR4, a 3'-5' poly(A) RNA and ssDNA exonuclease, is the catalytic component of the cytoplasmic deadenylase. *EMBO J.* 2002 Mar 15; 21(6):1414-26.

Chen J, Rappsilber J, Chiang YC, Russell P, Mann M, Denis CL. Purification and characterization of the 1.0 MDa CCR4-NOT complex identifies two novel components of the complex. *J Mol Biol.* 2001 Dec 7; 314(4):683-94.

Collins SR, Kemmeren P, Zhao XC, Greenblatt JF, Spencer F, Holstege FC, Weissman JS, Krogan NJ. Toward a comprehensive atlas of the physical interactome of *Saccharomyces cerevisiae*. *Mol Cell Proteomics.* 2007 Mar; 6(3):439-50.

Decker CJ, Parker R. A turnover pathway for both stable and unstable mRNAs in yeast: evidence for a requirement for deadenylation. *Genes Dev.* 1993 Aug; 7(8):1632-43.

Denis CL, Chiang YC, Cui Y, Chen J. Genetic evidence supports a role for the yeast CCR4-NOT complex in transcriptional elongation. *Genetics.* 2001 Jun; 158 (2): 627-34.

- Denis CL. Identification of new genes involved in the regulation of yeast alcohol dehydrogenase II. *Genetics*. 1984 Dec; 108(4):833-44.
- Deo RC, Bonanno JB, Sonenberg N, Burley SK. Recognition of polyadenylate RNA by the poly(A)-binding protein. *Cell*. 1999 Sep 17; 98(6):835-45.
- Derry MC, Yanagiya A, Martineau Y, Sonenberg N. Regulation of poly(A)-binding protein through PABP-interacting proteins. *Cold Spring Harb Symp Quant Biol*. 2006; 71:537-43.
- Dunckley T, Tucker M, Parker R. Two related proteins, Edc1p and Edc2p, stimulate mRNA decapping in *Saccharomyces cerevisiae*. *Genetics*. 2001 Jan; 157(1):27-37.
- Duttagupta R, Tian B, Wilusz CJ, Khounh DT, Soteropoulos P, Ouyang M, Dougherty JP, Peltz SW. Global analysis of Pub1p targets reveals a coordinate control of gene expression through modulation of binding and stability. *Mol Cell Biol*. 2005 Jul; 25(13):5499-513.
- Entrez Gene: PABPC4 poly(A) binding protein, cytoplasmic 4 (inducible form).
- Fekete CA, Applefield DJ, Blakely SA, Shirokikh N, Pestova T, Lorsch JR, Hinnebusch AG. The eIF1A C-terminal domain promotes initiation complex assembly, scanning and AUG selection in vivo. *EMBO J*. 2005 Oct 19; 24(20):3588-601.
- Fleischer TC, Weaver CM, McAfee KJ, Jennings JL, Link AJ. Systematic identification and functional screens of uncharacterized proteins associated with eukaryotic ribosomal complexes. *Genes Dev*. 2006 May 15; 20(10):1294-307.
- Gavin AC, Bösch M, Krause R, Grandi P, Marzioch M, Bauer A, Schultz J, Rick JM, Michon AM, Cruciat CM, Remor M, Höfert C, Schelder M, Brajenovic M, Ruffner H, Merino A, Klein K, Hudak M, Dickson D, Rudi T, Gnau V, Bauch A, Bastuck S, Huhse B, Leutwein C, Heurtier MA, Copley RR, Edelmann A, Querfurth E, Rybin V, Drewes G, Raida M, Bouwmeester T, Bork P, Seraphin B, Kuster B, Neubauer G, Superti-Furga G. Functional organization of the yeast proteome by systematic analysis of protein complexes. *Nature*. 2002 Jan 10; 415(6868):141-7.

Gorgoni B, Gray NK. The roles of cytoplasmic poly(A)-binding proteins in regulating gene expression: a developmental perspective. *Brief Funct Genomic Proteomic*. 2004 Aug; 3(2):125-41.

Harris MN, Ozpolat B, Abdi F, Gu S, Legler A, Mawuenyega KG, Tirado-Gomez M, Lopez-Berestein G, Chen X. Comparative proteomic analysis of *all-trans-retinoic acid* treatment reveals systematic posttranscriptional control mechanisms in acute promyelocytic leukemia. *Blood*. 2004 Sep 1; 104(5):1314-23.

Hershey JWB and Merrick WC. Pathway and mechanism of initiation of protein synthesis, p. 33–88. *In* N. Sonenberg, J. W. B. Hershey, and M. B. Mathews (ed.), *Translational control of gene expression*. Cold Spring Harbor Laboratory Press, 2000.

Hinnebusch, A.G. Translational regulation of GCN4 and the general amino acid control of yeast. *Annu Rev Microbiol*. 2005; 59:407-50.

Ho Y, Gruhler A, Heilbut A, Bader GD, Moore L, Adams SL, Millar A, Taylor P, Bennett K, Boutilier K, Yang L, Wolting C, Donaldson I, Schandorff S, Shewnarane J, Vo M, Taggart J, Goudreault M, Muskat B, Alfarano C, Dewar D, Lin Z, Michalickova K, Willems AR, Sassi H, Nielsen PA, Rasmussen KJ, Andersen JR, Johansen LE, Hansen LH, Jespersen H, Podtelejnikov A, Nielsen E, Crawford J, Poulsen V, Sørensen BD, Matthiesen J, Hendrickson RC, Gleeson F, Pawson T, Moran MF, Durocher D, Mann M, Hogue CW, Figeys D, Tyers M. Systematic identification of protein complexes in *Saccharomyces cerevisiae* by mass spectrometry. *Nature*. 2002 Jan 10; 415(6868):180-3.

Hogan DJ, Riordan DP, Gerber AP, Herschlag D, Brown PO. Diverse RNA-binding proteins interact with functionally related sets of RNAs, suggesting an extensive regulatory system. *PLoS Biol*. 2008 Oct 28; 6(10):e255.

Howlett GJ, Minton AP, Rivas G. Analytical ultracentrifugation for the study of protein association and assembly. *Curr Opin Chem Biol*. 2006 Oct; 10(5):430-6.

Ibeas JI, Yun DJ, Damsz B, Narasimhan ML, Uesono Y, Ribas JC, Lee H, Hasegawa PM, Bressan RA, Pardo JM. Resistance to the plant PR-5 protein osmotin in the model fungus *Saccharomyces cerevisiae* is mediated by the regulatory effects of SSD1 on cell wall composition. *Plant J*. 2001 Feb; 25(3):271-80.

Ibrahimo, S., L.E. Holmes, and M.P. Ashe. Regulation of translation initiation by the yeast eIF4E binding proteins is required for the pseudohyphal response. *Yeast*. 2006 Oct-Nov; 23(14-15):1075-88.

Jansen JM, Wanless AG, Seidel CW, Weiss EL. Cbk1 regulation of the RNA-binding protein Ssd1 integrates cell fate with translational control. *Curr Biol*. 2009 Dec 29; 19(24):2114-20.

Jivotovskaya AV, Valásek L, Hinnebusch AG, Nielsen KH. Eukaryotic translation initiation factor 3 (eIF3) and eIF2 can promote mRNA binding to 40S subunits independently of eIF4G in yeast. *Mol Cell Biol*. 2006 Feb; 26(4):1355-72.

Kanaan AS, Frank F, Maedler-Kron C, Verma K, Sonenberg N, Nagar B. Crystallization and preliminary X-ray diffraction analysis of the middle domain of Paip1. *Acta Crystallogr Sect F Struct Biol Cryst Commun*. 2009 Oct 1; 65 (Pt 10):1060-4.

Kapp, L.D., and J.R. Lorsch. The molecular mechanics of eukaryotic translation. *Annu Rev Biochem*. 2004; 73:657-704.

Katz L, Burge CB. Widespread selection for local RNA secondary structure in coding regions of bacterial genes. *Genome Res*. 2003 Sep; 13(9):2042-51.

Kim JH, Richter JD. RINGO/cdk1 and CPEB mediate poly (A) tail stabilization and translational regulation by ePAB. *Genes Dev*. 2007 Oct 15; 21(20):2571-9.

Kolupaeva VG, Unbehauen A, Lomakin IB, Hellen CU, Pestova TV. Binding of eukaryotic initiation factor 3 to ribosomal 40S subunits and its role in ribosomal dissociation and antiassociation. *RNA*. 2005 Apr; 11(4):470-86.

Kozlov G, Trempe JF, Khaleghpour K, Kahvejian A, Ekiel I, Gehring K. Structure and function of the C-terminal PABC domain of human poly(A)-binding protein. *Proc Natl Acad Sci U S A*. 2001 Apr 10; 98(8):4409-13.

Kroe, R. Application of fluorescence detected sedimentation. Ph.D. Thesis, University of New Hampshire. 2005.

Krogan NJ, Cagney G, Yu H, Zhong G, Guo X, Ignatchenko A, Li J, Pu S, Datta N, Tikuisis AP, Punna T, Peregrín-Alvarez JM, Shales M, Zhang X,

Davey M, Robinson MD, Paccanaro A, Bray JE, Sheung A, Beattie B, Richards DP, Canadien V, Lalev A, Mena F, Wong P, Starostine A, Canete MM, Vlasblom J, Wu S, Orsi C, Collins SR, Chandran S, Haw R, Rilstone JJ, Gandi K, Thompson NJ, Musso G, St Onge P, Ghanny S, Lam MH, Butland G, Altaf-Ul AM, Kanaya S, Shilatifard A, O'Shea E, Weissman JS, Ingles CJ, Hughes TR, Parkinson J, Gerstein M, Wodak SJ, Emili A, Greenblatt JF. Global landscape of protein complexes in the yeast *Saccharomyces cerevisiae*. *Nature*. 2006 Mar 30; 440(7084):637-43.

Kühn U, Pieler T. *Xenopus* poly (A) binding protein: functional domains in RNA binding and protein-protein interaction. *J Mol Biol*. 1996 Feb 16; 256(1):20-30.

Laue TM, Stafford WF 3rd. Modern applications of analytical ultracentrifugation. *Annu Rev Biophys Biomol Struct*. 1999; 28:75-100.

Laue TM, Stafford WF 3rd. Modern applications of analytical ultracentrifugation. *Annu Rev Biophys Biomol Struct*. 1999; 28:75-100.

Laue TM. Sedimentation equilibrium as thermodynamic tool. *Methods Enzymol*. 1995; 259:427-52.

Lee D, Ohn T, Chiang YC, Quigley G, Yao G, Liu Y, Denis CL. PUF3 acceleration of deadenylation in vivo can operate independently of CCR4 activity, possibly involving effects on the PAB1-mRNP structure. *J Mol Biol*. 2010 Jun 18;399(4):562-75.

Lindstein T, June CH, Ledbetter JA, Stella G, Thompson CB. Regulation of lymphokine messenger RNA stability by a surface-mediated T cell activation pathway. *Science*. 1989 Apr 21; 244 (4902):339-43.

López de Silanes I, Lal A, Gorospe M. HuR: post-transcriptional paths to malignancy. *RNA Biol*. 2005 Jan; 2(1):11-3.

Maag D, Lorsch JR. Communication between eukaryotic translation initiation factors 1 and 1A on the yeast small ribosomal subunit. *J Mol Biol*. 2003 Jul 25; 330(5):917-24.

MacGregor IK, Anderson AL, Laue TM. Fluorescence detection for the XLI analytical ultracentrifuge. *Biophys Chem*. 2004 Mar 1; 108(1-3):165-85.

Mangus DA, Amrani N, Jacobson A. Pbp1p, a factor interacting with *Saccharomyces cerevisiae* poly(A)-binding protein, regulates polyadenylation. *Mol Cell Biol.* 1998 Dec; 18(12):7383-96.

McLafferty FW, Breuker K, Jin M, Han X, Infusini G, Jiang H, Kong X, Begley TP. Top-down MS, a powerful complement to the high capabilities of proteolysis proteomics. *FEBS J.* 2007 Dec; 274(24):6256-68.

McMahon RJ, Frost SC. Nutrient control of GLUT1 processing and turnover in 3T3-L1 adipocytes. *J Biol Chem.* 1995 May 19; 270(20):12094-9.

Miluzio A, Beugnet A, Volta V, Biffo S. Eukaryotic initiation factor 6 mediates a continuum between 60S ribosome biogenesis and translation. *EMBO Rep.* 2009 May; 10(5):459-65.

Mitchell P, Petfalski E, Shevchenko A, Mann M, Tollervey D. The exosome: a conserved eukaryotic RNA processing complex containing multiple 3'→5' exoribonucleases. *Cell.* 1997 Nov 14; 91(4):457-66.

Mix H, Lobanov AV, Gladyshev VN. SECIS elements in the coding regions of selenoprotein transcripts are functional in higher eukaryotes. *Nucleic Acids Res.* 2007; 35(2):414-23.

Muhlrad D, Decker CJ, Parker R. Deadenylation of the unstable mRNA encoded by the yeast MFA2 gene leads to decapping followed by 5'→3' digestion of the transcript. *Genes Dev.* 1994 Apr 1; 8(7):855-66.

Mullin C, Duning K, Barnekow A, Richter D, Kremerskothen J, Mohr E. Interaction of rat poly(A)-binding protein with poly(A)- and non-poly(A) sequences is preferentially mediated by RNA recognition motifs 3+4. *FEBS Lett.* 2004 Oct 22; 576(3):437-41.

Niehhs C, Pollet N. Synexpression groups in eukaryotes. *Nature.* 1999 Dec 2; 402 (6761):483-7.

Ohyama Y, Kasahara K, Kokubo T. *Saccharomyces cerevisiae* Ssd1p promotes CLN2 expression by binding to the 5'-untranslated region of CLN2 mRNA. *Genes Cells.* 2010 Oct 26. Epub ahead of print.

Ormö M, Cubitt AB, Kallio K, Gross LA, Tsien RY, Remington SJ. Crystal structure of the *Aequorea victoria* green fluorescent protein. *Science.* 1996 Sep 6; 273(5280):1392-5.

- Otero LJ, Ashe MP, Sachs AB. The yeast poly(A)-binding protein Pab1p stimulates in vitro poly(A)-dependent and cap-dependent translation by distinct mechanisms. *EMBO J*. 1999 Jun 1; 18 (11):3153-63.
- Pain VM. Initiation of protein synthesis in eukaryotic cells. *Eur J Biochem*. 1996 Mar 15; 236(3):747-71.
- Park MH. The post-translational synthesis of a polyamine-derived amino acid, hypusine, in the eukaryotic translation initiation factor 5A (eIF5A). *J Biochem*. 2006 Feb; 139(2):161-9.
- Parker R, Sheth U. P bodies and the control of mRNA translation and degradation. *Mol Cell*. 2007 Mar 9; 25(5):635-46.
- Parker R, Sheth U. P bodies and the control of mRNA translation and degradation. *Mol Cell*. 2007 Mar 9; 25(5):635-46.
- Pelham HR, Jackson RJ. An efficient mRNA-dependent translation system from reticulocyte lysates. *Eur J Biochem*. 1976 Aug 1; 67(1):247-56.
- Pestova TV, Hellen CU. Ribosome recruitment and scanning: what's new? *Trends Biochem Sci*. 1999 Mar; 24(3):85-7.
- Pestova TV, Lomakin IB, Lee JH, Choi SK, Dever TE, Hellen CU. The joining of ribosomal subunits in eukaryotes requires eIF5B. *Nature*. 2000 Jan 20; 403(6767):332-5.
- Phan L, Zhang X, Asano K, Anderson J, Vornlocher HP, Greenberg JR, Qin J, Hinnebusch AG. Identification of a translation initiation factor 3 (eIF3) core complex, conserved in yeast and mammals, that interacts with eIF5. *Mol Cell Biol*. 1998 Aug; 18(8):4935-46.
- Piecyk M, Wax S, Beck AR, Kedersha N, Gupta M, Maritim B, Chen S, Gueydan C, Krusys V, Streuli M, Anderson P. TIA-1 is a translational silencer that selectively regulates the expression of TNF-alpha. *EMBO J*. 2000 Aug 1; 19(15):4154-63.
- R.Jackson. Alternative mechanisms of initiating translation of mammalian mRNAs. *Biochem Soc Trans*. 2005 Dec; 33(Pt 6):1231-41.
- Reguly T, Breitkreutz A, Boucher L, Breitkreutz BJ, Hon GC, Myers CL, Parsons A, Friesen H, Oughtred R, Tong A, Stark C, Ho Y, Botstein D,

Andrews B, Boone C, Troyanskya OG, Ideker T, Dolinski K, Batada NN, Tyers M. Comprehensive curation and analysis of global interaction networks in *Saccharomyces cerevisiae*. *J Biol.* 2006; 5(4):11.

Roll-Mecak A, Alone P, Cao C, Dever TE, Burley SK. X-ray structure of translation initiation factor eIF2gamma: implications for tRNA and eIF2alpha binding. *J Biol Chem.* 2004 Mar 12; 279(11):10634-42.

Roy G, De Crescenzo G, Khaleghpour K, Kahvejian A, O'Connor-McCourt M, Sonenberg N. Paip1 interacts with poly(A) binding protein through two independent binding motifs. *Mol Cell Biol.* 2002 Jun; 22(11):3769-82.

Sachs AB, Bond MW, Kornberg RD. A single gene from yeast for both nuclear and cytoplasmic polyadenylate-binding proteins: domain structure and expression. *Cell.* 1986 Jun 20; 45(6):827-35.

Sachs AB, Davis RW, and Kornberg RD. A single domain of yeast poly (A)-binding protein is necessary and sufficient for RNA binding and cell viability. *Mol Cell Biol.* 1987 September; 7(9): 3268-3276.

Sanvito F, Vivoli F, Gambini S, Santambrogio G, Catena M, Viale E, Veglia F, Donadini A, Biffo S, Marchisio PC. Expression of a highly conserved protein, p27BBP, during the progression of human colorectal cancer. *Cancer Res.* 2000 Feb 1; 60(3):510-6.

Sarah F. Mitchell and Jon R. Lorsch. Should I Stay or Should I Go? Eukaryotic Translation Initiation Factors 1 and 1A Control Start Codon Recognition. *J Biol Chem.* 2008 October 10; 283(41): 27345–27349.

Schwartz D, Decker CJ Parker R. The enhancer of decapping proteins, Edc1p and Edc2p, bind RNA and stimulate the activity of the decapping enzyme. *RNA.* 2003 Feb; 9(2):239-51.

Scott DJ, and Schuck P. A brief introduction to the analytical ultracentrifugation of proteins for beginners. In "Analytical Ultracentrifugation". 2005; pp. 1–25. Royal Society of Chemistry, Cambridge, UK.

Segal SP, Dunckley T, Parker R. Sbp1p affects translational repression and decapping in *Saccharomyces cerevisiae*. *Mol Cell Biol.* 2006 Jul; 26(13):5120-30.

Shabalina SA, Ogurtsov AY, Spiridonov NA. *A periodic pattern of mRNA secondary structure created by the genetic code. Nucleic Acids Res. 2006 May 8; 34(8):2428-37.*

Sheth U, Parker R. Decapping and decay of messenger RNA occur in cytoplasmic processing bodies. *Science. 2003 May 2; 300(5620):805-8.*

SHIMOMURA O, JOHNSON FH, SAIGA Y. Extraction, purification and properties of aequorin, a bioluminescent protein from the luminous hydromedusan, *Aequorea*. *J Cell Comp Physiol. 1962 Jun;59:223-39.*

Sobel SG, Wolin SL. Two yeast La motif-containing proteins are RNA-binding proteins that associate with polyribosomes. *Mol Biol Cell. 1999 Nov; 10(11):3849-62.*

Tarun SZ Jr, Sachs AB. Association of the yeast poly (A) tail binding protein with translation initiation factor eIF-4G. *EMBO J. 1996 Dec 16; 15(24):7168-77.*

Tatyana VP, Kolupaeva VG, Lomakin IB, Pilipenko EV, Shatsky IN, Agol VI, Hellen CU. Molecular mechanisms of translation initiation in eukaryotes. *Proc Natl Acad Sci U S A. 2001 Jun 19; 98(13):7029-36.*

Tsien RY. The green fluorescent protein. *Annu Rev Biochem. 1998; 67:509-44.*
Tucker M, Staples RR, Valencia-Sanchez MA, Muhlrads D, Parker R. Ccr4p is the catalytic subunit of a Ccr4p/Pop2p/Notp mRNA deadenylase complex in *Saccharomyces cerevisiae*. *EMBO J. 2002 Mar 15; 21(6):1427-36.*

Uchida N, Hoshino S, Imataka H, Sonenberg N, Katada T. A novel role of the mammalian GSPT/eRF3 associating with poly(A)-binding protein in Cap/Poly(A)-dependent translation. *J Biol Chem. 2002 Dec 27; 277(52):50286-92.*

Unbehauen A, Borukhov SI, Hellen CU, Pestova TV. Release of initiation factors from 48S complexes during ribosomal subunit joining and the link between establishment of codon-anticodon base-pairing and hydrolysis of eIF2-bound GTP. *Genes Dev. 2004 Dec 15; 18(24):3078-93.*

Valásek L, Szamecz B, Hinnebusch AG, Nielsen KH. In vivo stabilization of preinitiation complexes by formaldehyde cross-linking. *Methods Enzymol. 2007; 429:163-83.*

Van den Heuvel J, Lang V, Richter G, Price N, Peacock L, Proud C, McCarthy JE. The highly acidic C-terminal region of the yeast initiation factor

subunit 2 α (eIF-2 α) contains casein kinase phosphorylation sites and is essential for maintaining normal regulation of GCN4 *Biochim Biophys Acta*. 1995 Apr 26; 1261(3):337-48.

Viswanathan P, Ohn T, Chiang YC, Chen J, Denis CL. Mouse CAF1 can function as a processive deadenylase/3'-5'-exonuclease in vitro but in yeast the deadenylase function of CAF1 is not required for mRNA poly(A) removal. *J Biol Chem*. 2004 Jun 4;279 (23): 23988-95.

Voeltz GK, Ongkasuwan J, Standart N, Steitz JA. A novel embryonic poly (A) binding protein, ePAB, regulates mRNA deadenylation in *Xenopus* egg extracts. *Genes Dev*. 2001 Mar 15;15(6):774-88.

Von der Haar T, Gross JD, Wagner G, McCarthy JE. The mRNA cap-binding protein eIF4E in post-transcriptional gene expression. *Nat Struct Mol Biol*. 2004 Jun; 11(6):503-11.

Wachter A. Riboswitch-mediated control of gene expression in eukaryotes. *RNA Biol*. 2010 Jan-Feb;7(1):67-76

Walther TC, Mann M. Mass spectrometry-based proteomics in cell biology. *J Cell Biol*. 2010 Aug 23; 190(4):491-500.

Wells SE, Hillner PE, Vale RD, Sachs AB. Circularization of mRNA by eukaryotic translation initiation factors. *Mol. Cell* 1998; 2:135–140.

Yang F, Moss LG, Phillips GN Jr. The molecular structure of green fluorescent protein. *Nat Biotechnol*. 1996 Oct; 14(10):1246-51.

Yao G, Chiang YC, Zhang C, Lee DJ, Laue TM, Denis CL. PAB1 self-association precludes its binding to poly(A), thereby accelerating CCR4 deadenylation in vivo. *Mol Cell Biol*. 2007 Sep; 27(17):6243-53.

Yu W, Farrell RA, Stillman DJ, Winge DR. Identification of SLF1 as a new copper homeostasis gene involved in copper sulfide mineralization in *Saccharomyces cerevisiae*. *Mol Cell Biol*. 1996 May; 16(5):2464-72.

Zhouravleva G, Frolova L, Le Goff X, Le Guellec R, Inge-Vechtomov S, Kisselev L, Philippe M. Termination of translation in eukaryotes is governed by two interacting polypeptide chain release factors, eRF1 and eRF3. *EMBO J*. 1995 Aug 15; 14(16):4065-72.